JVI Journals.ASM.org

Interleukin-1- and Type I Interferon-Dependent Enhanced Immunogenicity of an NYVAC-HIV-1 Env-Gag-Pol-Nef Vaccine Vector with Dual Deletions of Type I and Type II Interferon-Binding Proteins

Julie Delaloye,[a] Abdelali Filali-Mouhim,[b] Mark J. Cameron,[b] Elias K. Haddad,[b] Alexandre Harari,[c] Jean-Pierre Goulet,[b] Carmen E. Gomez,[d] Beatriz Perdiguero,[d] Mariano Esteban,[d] Giuseppe Pantaleo,[c] Thierry Roger,[a] Rafick-Pierre Sékaly,[b] Thierry Calandra[a]

Infectious Diseases Service[a] and Division of Immunology and Allergy,[c] Centre Hospitalier Universitaire Vaudois, and University of Lausanne, Lausanne, Switzerland; Vaccine and Gene Therapy Institute, Port St. Lucie, Florida, USA[b]; Centro Nacional de Biotecnología, CSIC, Madrid, Spain[d]

ABSTRACT

NYVAC, a highly attenuated, replication-restricted poxvirus, is a safe and immunogenic vaccine vector. Deletion of immune evasion genes from the poxvirus genome is an attractive strategy for improving the immunogenic properties of poxviruses. Using systems biology approaches, we describe herein the enhanced immunological profile of NYVAC vectors expressing the HIV-1 clade C *env*, *gag*, *pol*, and *nef* genes (NYVAC-C) with single or double deletions of genes encoding type I (Δ*B19R*) or type II (Δ*B8R*) interferon (IFN)-binding proteins. Transcriptomic analyses of human monocytes infected with NYVAC-C, NYVAC-C with the *B19R* deletion (NYVAC-C-ΔB19R), or NYVAC-C with *B8R* and *B19R* deletions (NYVAC-C-ΔB8RB19R) revealed a concerted upregulation of innate immune pathways (IFN-stimulated genes [ISGs]) of increasing magnitude with NYVAC-C-ΔB19R and NYVAC-C-ΔB8RB19R than with NYVAC-C. Deletion of *B8R* and *B19R* resulted in an enhanced activation of IRF3, IRF7, and STAT1 and the robust production of type I IFNs and of ISGs, whose expression was inhibited by anti-type I IFN antibodies. Interestingly, NYVAC-C-ΔB8RB19R induced the production of much higher levels of proinflammatory cytokines (tumor necrosis factor [TNF], interleukin-6 [IL-6], and IL-8) than NYVAC-C or NYVAC-C-ΔB19R as well as a strong inflammasome response (caspase-1 and IL-1β) in infected monocytes. Top network analyses showed that this broad response mediated by the deletion of *B8R* and *B19R* was organized around two upregulated gene expression nodes (TNF and IRF7). Consistent with these findings, monocytes infected with NYVAC-C-ΔB8RB19R induced a stronger type I IFN-dependent and IL-1-dependent allogeneic $CD4^+$ T cell response than monocytes infected with NYVAC-C or NYVAC-C-ΔB19R. Dual deletion of type I and type II IFN immune evasion genes in NYVAC markedly enhanced its immunogenic properties via its induction of the increased expression of type I IFNs and IL-1β and make it an attractive candidate HIV vaccine vector.

IMPORTANCE

NYVAC is a replication-deficient poxvirus developed as a vaccine vector against HIV. NYVAC expresses several genes known to impair the host immune defenses by interfering with innate immune receptors, cytokines, or interferons. Given the crucial role played by interferons against viruses, we postulated that targeting the type I and type II decoy receptors used by poxvirus to subvert the host innate immune response would be an attractive approach to improve the immunogenicity of NYVAC vectors. Using systems biology approaches, we report that deletion of type I and type II IFN immune evasion genes in NYVAC poxvirus resulted in the robust expression of type I IFNs and interferon-stimulated genes (ISGs), a strong activation of the inflammasome, and upregulated expression of IL-1β and proinflammatory cytokines. Dual deletion of type I and type II IFN immune evasion genes in NYVAC poxvirus improves its immunogenic profile and makes it an attractive candidate HIV vaccine vector.

The control of human immunodeficiency virus (HIV) transmission is a public health priority, and considerable resources and efforts have been dedicated to HIV vaccine research. The ideal HIV vaccine should elicit both humoral and cellular effector functions to induce durable protective immunity (1, 2). One approach used to generate robust T cell responses is to express HIV antigens in recombinant replication-defective viral vaccine vectors, such as adenovirus or poxvirus (3). In recent years, adenovirus vectors based on human adenovirus serotype 5 (Ad5) have become a promising platform for HIV vaccine development (4). However, the Step Ad5 HIV-1 gag/pol/nef vaccine trials failed to prevent HIV-1 infection or to reduce the early viral load in Ad5-seronegative subjects. More importantly, it was associated with an increased rate of HIV infection in individuals with preexisting immunity to Ad5 (5). Two other trials of a recombinant Ad5-vectored HIV-1 vaccine, the HVTN 503 and the HVTN 505 trials, did not show vaccine efficacy (6–8).

Poxviruses offer a promising alternative to adenoviruses, as illustrated by the results of the phase III Thai HIV prime-boost vaccine study combining a live recombinant canarypox vaccine vector (ALVAC-HIV) and a glycoprotein 120 subunit vaccine (AIDSVAX B/E) (9). This vaccine regimen was well tolerated and had a definitive, albeit modest (31%) efficacy for the prevention of HIV infection. However, it did not change the levels of viremia or increase $CD4^+$ T cell counts in subjects who developed HIV-1 infection. Regardless of these encouraging results, the search must thus go on to develop new poxvirus-based vaccine vectors with improved clinical efficacy.

Poxviruses have been studied extensively as gene transfer vectors (10). A large packaging capacity for recombinant DNA, precise virus-specific control of target gene expression, a lack of persistence of genomic integration in the host, and high immunogenicity when used as a vaccine make poxviruses very attractive as gene delivery systems for the development of new vaccines (11). Vaccinia virus (VACV) was one of the poxviruses used for recombinant gene expression. Concerns about the safety of VACV led to the development of highly attenuated strains of poxviruses, such as ALVAC, MVA, and NYVAC. NYVAC is a derivative of the Copenhagen VACV strain with attenuated virulence due to the deletion of 18 open reading frames involved in host tropism, virulence, and pathogenesis (12). NYVAC vectors are replication deficient in most mammalian cells and have been shown to be safe and immunogenic in humans (13). These favorable intrinsic properties have made NYVAC an interesting virus vector for use in a vaccine against HIV and other pathogens causing infectious diseases. NYVAC vectors expressing either the simian immunodeficiency virus (SIV) or the HIV type 1 (HIV-1) *env*, *gag*, *pol*, and *nef* genes have been shown to exhibit favorable immunological and safety profiles in preclinical and clinical studies (14–16). Recent studies showed that a DNA-C prime and NYVAC-C boost regimen induced HIV-specific $CD4^+$ and $CD8^+$ T cell responses in the blood and intestinal mucosa of healthy vaccinees (15, 17, 18). Moreover, polyfunctional HIV-specific T cell responses were observed in chronically infected, antiretroviral therapy-treated HIV-infected patients following NYVAC immunization (17).

Notwithstanding these promising results, there is a clear need to design novel NYVAC vaccine vectors with improved immunological profiles. To achieve this goal, NYVAC vectors were generated using a recombinant virus expressing HIV-1 clade C *env*, *gag*, *pol*, and *nef* genes (NYVAC-C) and single or multiple deletions of critical immune evasion genes known to impair the host innate immune defense response by interference with Toll-like receptor (TLR) sensing pathways, cytokines, or interferons (IFNs) (19, 20).

Given the crucial role played by the IFN family of cytokines in the modulation of host innate and adaptive immune responses against viruses, targeting of either type I (alpha IFN [IFN-α], IFN-β) or type II (IFN-γ) decoy receptors released by poxvirus appeared to be an attractive approach to improve the immunogenicity of NYVAC. Here we report on systems biology approaches used to characterize the enhanced immunological profile of an NYVAC-C vaccine vector with the deletion of a single gene (Δ*B19R*) or two genes (Δ*B8R* Δ*B19R*) encoding soluble proteins binding to and inhibiting type I (B19) or type II (B8) IFN binding to their cognate receptors.

Received 28 October 2014 **Accepted** 12 January 2015

Accepted manuscript posted online 21 January 2015

Citation Delaloye J, Filali-Mouhim A, Cameron MJ, Haddad EK, Harari A, Goulet J-P, Gomez CE, Perdiguero B, Esteban M, Pantaleo G, Roger T, Sékaly R-P, Calandra T. 2015. Interleukin-1- and type I interferon-dependent enhanced immunogenicity of an NYVAC-HIV-1 Env-Gag-Pol-Nef vaccine vector with dual deletions of type I and type II interferon-binding proteins. J Virol 89:3819–3832. doi:10.1128/JVI.03061-14.

Editor: G. Silvestri

Address correspondence to Thierry Calandra, Thierry.Calandra@chuv.ch.

J.D. and A.F.-M. contributed equally to this article.

Supplemental material for this article may be found at http://dx.doi.org/10.1128/JVI.03061-14.

doi:10.1128/JVI.03061-14

MATERIALS AND METHODS

Ethics statement. Blood samples from healthy subjects were obtained from the blood bank of Lausanne, Switzerland. Donors provided written consent, and all samples were processed anonymously.

Cells and reagents. Peripheral blood mononuclear cells from healthy donors (recruited by the Blood Center, Lausanne, Switzerland) were obtained by use of a Ficoll-Hypaque density gradient (GE Healthcare, Glattbrugg, Switzerland). Human primary monocytes (purity, >97%) were isolated using anti-CD14 beads (Miltenyi Biotech, Bergisch Gladbach, Germany), whereas $CD4^+$ T cells (purity, 95%) were isolated using the human CD4 T lymphocyte enrichment set-DM (BD Biosciences, Erembodegem, Belgium). Cells of the human monocytic THP-1 cell line (American Type Culture Collection, Manassas, VA) were cultured in RPMI 1640 medium containing 2 mM L-glutamine, 50 μM 2-mercaptoethanol, 100 IU/ml of penicillin, and 100 μg/ml of streptomycin (all from Invitrogen, San Diego, CA) plus 10% heat-inactivated fetal calf serum (Sigma-Aldrich, St. Louis, MO). THP-1 cells were differentiated into macrophages by treatment for 24 h with 65 ng/ml phorbol 12-myristate 13-acetate (PMA; Sigma-Aldrich) before usage. In selected experiments, cells were incubated with 10 μg/ml of human anti-IFN-α (clone MMHA-2) plus anti-IFN-β (clone MMHB-2) control antibody (both clones were from PBL Biomedical Laboratories, Piscataway, NJ) or 100 μg/ml of recombinant human interleukin-1 (IL-1) receptor antagonist (IL-1ra; R&D Systems, Minneapolis, MN).

Production of NYVAC vaccine vectors and *in vitro* models of infection. NYVAC-C poxviruses expressing the HIV-1 clade C *env*, *gag*, *pol*, and *nef* genes were cultured in chicken embryo fibroblasts, purified by two sucrose cushions, and titrated on BHK-21 and BSC-40 cells as previously described (21). NYVAC-C was used to generate NYVAC-C vectors with a *B19R* single deletion (NYVAC-C-ΔB19R) or a *B8R* and *B19R* double deletion (NYVAC-C-ΔB8RB19R) as described elsewhere (20, 22, 23). Human primary monocytes and THP-1 cells were infected for 1 h with the NYVAC-C, NYVAC-C-ΔB19R, or NYVAC-C-ΔB8RB19R vectors at a multiplicity of infection (MOI) of 1 or 5 PFU/cell. Cell culture medium was removed, and incubation was continued to the chosen time point. Cells and cell culture supernatants were then collected and processed for enzyme-linked immunosorbent assay (ELISA), RNA extraction, and Western blot analyses. For whole-blood assay, 100 μl of heparinized whole blood from healthy subjects was diluted 5-fold in RPMI 1640 medium containing the NYVAC vectors and incubated for 24 h at 37°C in the presence of 5% CO_2 (21). Cell-free supernatants were harvested and stored at −80°C until measurement of cytokine levels.

Gene expression analysis. Microarray analysis was performed on primary cells from a total of 4 donors as previously described (24). Briefly, RNA was isolated using RNeasy microkits (Qiagen, Hombrechtikon, Switzerland). The quantity and quality of the RNA were evaluated using a NanoDrop 2000c spectrophotometer (NanoDrop Technologies, Willington, DE) and an Experion electrophoresis system (Bio-Rad, Hercules, CA). Total RNA (50 ng) was amplified using Illumina TotalPrep RNA amplification kits (Life Technologies, Grand Island, NY). Biotinylated cRNA (750 ng) was hybridized onto HumanHT-12_V4 BeadChips and quantified using an Illumina BeadStation 500GX scanner and Illumina BeadScan software. Gene expression data were preprocessed using R and Bioconductor software (24, 25). The LIMMA package was used to fit a linear model to each probe and perform (moderated) *t* tests or *F* tests on the groups being compared. To control the expected proportions of false-positive results, the false discovery rate for each unadjusted *P* value was calculated using the Benjamini and Hochberg method implemented in LIMMA.

Pathway and network analysis was used to identify canonical signaling pathways and molecular interaction networks from a list of genes selected as being differentially expressed between two groups of samples using Ingenuity

Pathway Analysis (IPA) software (Ingenuity Systems, Redwood City, CA) (26). Genes that had adjusted *P* values of <0.25 and absolute fold change (FC) values of >1.3 were used for pathway and network analysis. General IFN response genes were filtered on the basis of a published list (27) and our own supplementation (24). The resulting general IFN responses were also filtered for genes unique or common to type I (IFN-α) and type II (IFN-γ) responses via a query based on published IFN-α and IFN-γ gene lists from Waddell et al. (27) and additional curation and annotation supplied by the GeneCards (http://www.genecards.org) and NCBI Biosystems (http://www.ncbi.nlm.nih.gov/biosystems) public databases (see Table S1 in the supplemental material).

Real-time PCR. Real-time PCR analyses were performed as previously described (24). Briefly, 1 μg of total RNA was reverse transcribed using a SuperScript VILO cDNA synthesis kit (Invitrogen) with random primers. The cDNA was analyzed in duplicate on an OpenArray NT cycler (BioTrove) using TaqMan real-time PCR plates (Applied Biosystems, Rotkreuz, Switzerland) preloaded with primer pairs (see Table S2 in the supplemental material). cDNA samples were loaded into the plates using an OpenArray AccuFill instrument (Applied Biosystems) according to the manufacturer's protocols. Each subarray was loaded with 2.5 μl 2× GeneAmp Fast PCR master mix (Applied Biosystems), 1 μl 5× TaqMan OpenArray remix (Applied Biosystems), 0.3 μl RNase-free water, and 1.2 μl cDNA. For the thermal cycling protocol, the manufacturer's default settings were used. mRNA levels were normalized using 4 housekeeping genes, glucose-6-phosphate dehydrogenase (G6PD), β_2-microglobulin (B2M), DnaJ homolog subfamily A member 4 (DNAJA4), and β-actin (ACTB), after transforming the threshold cycle (C_T) values into $-\Delta C_T$ values. The analysis was performed using R software.

The real-time PCR analyses whose results are presented in Fig. 8A were performed as described previously (21). Total RNA was isolated from THP-1 cells using an RNeasy kit (Qiagen, Hombrechtikon, Switzerland). Reverse transcription (RT) of 1 μg of RNA was performed using an ImProm-II reverse transcription system kit (Promega, Dübendorf, Switzerland). Quantitative PCR was performed with a 7500 Fast real-time PCR system (Applied Biosystems, Rotkreuz, Switzerland) using the Power SYBR green PCR master mix (Applied Biosystems). The following primers (5′-3′ sense and antisense primer sequences) were used for amplification: IFIT1 (TTGCCTGGATGTATTACCAC and GCTTCTTGCAAATGTTCTCC), IFIT2 (ACAAGGCCATCCACCACTTTAT and CCCAGCAATTCAGGTGTTAACA), CXCL10/IP-10 (CTGCTTTGGGGTTTATCAGA and CCACTGAAAGAATTTGGGC), IL-29 (GGACGCCTTGGAAGAGTCAC and ACTAGAAGCCTCAGGTCCCAATTCTTC), STAT1 (AAGGGGCCATCACATTCACA and GATACTTCAGGGGATTCTCT), and IRF7 (TGCAAGGTGTACTGGGAG and TCAAGCTTCTGCTCCAGCTCCATAAG). All samples were tested in triplicate. Amplifications consisted of a denaturation step at 95°C for 15 s and an annealing/extension step at 60°C for 60 s with the 9600 emulation mode. For each measurement, a standard made of successive dilutions of a reference cDNA was processed in parallel. The level of expression of specific genes was expressed relative to the level of expression of hypoxanthine phosphoribosyltransferase (HPRT) and is given in arbitrary units.

Western blot analysis. THP-1 cells were washed with ice-cold phosphate-buffered saline and lysed for 5 min at 4°C with the mammalian protein extraction reagent (Pierce Biotechnology Inc., Rockford, IL). Reaction mixtures were centrifuged for 5 min at 18,000 × *g*. The protein concentration of the supernatants was determined using a bicinchoninic acid protein assay (Pierce Biotechnology). Cell lysates were electrophoresed through 12% (wt/vol) polyacrylamide gels and transferred onto nitrocellulose membranes (Schleicher & Schuell, Keene, NH). Membranes were incubated with antibodies directed against phospho-IRF3 (P-IRF3; Cell Signaling Technology, Danvers, TX), phospho-STAT1 (P-STAT1) and total STAT1 (BD Biosciences), IRF7 (Zymed, San Francisco, CA), and tubulin (Sigma-Aldrich). After they were washed, the membranes were incubated with horseradish peroxidase (HRP)-conjugated secondary antibody (Pierce). Signals were revealed using an ECL Western blotting analysis system (GE Healthcare). Images were recorded using an ImageQuant LAS 4000 system (GE Healthcare).

Measurement of cytokine production. The concentrations of tumor necrosis factor (TNF) and IL-6 were measured by bioassay (28), whereas the concentrations of IL-1β (Bender MedSystems, Vienna, Austria), IL-8 (BD Biosciences), IFN-γ-induced protein 10 (IP-10) and macrophage inflammatory protein 1α (MIP-1α) (R&D Systems) and the concentrations of IFN-α and IFN-β (PBL Biomedical Laboratories, Piscataway, NJ) were measured by ELISA.

Mixed lymphocyte reactions. Human monocytes were infected for 18 h with NYVAC-C, NYVAC-C-ΔB19R, or NYVAC-C-ΔB8RB19R (MOIs, 0.1, 1, and 10). Supernatants were harvested and stored at −80°C until measurement of IFN-α levels. After washing, 5×10^5 monocytes were cocultured with allogeneic $CD4^+$ T cells at five distinct monocyte/$CD4^+$ T cell ratios (1/10, 1/20, 1/40, 1/80, 1/160) in a 96-well cell culture plate. After 5 days, cell cultures were pulsed with [^{3}H]thymidine (1.0 μCi per well). Proliferation was monitored by measuring the level of thymidine incorporation over 18 h.

Statistical analyses. Statistical analyses specific for gene expression analysis were performed as described above in "Gene expression analysis." Comparisons among treatment groups were performed by two-tailed paired Student's *t* test. *P* values of less than 0.05 were considered to indicate statistical significance.

Microarray data accession number. The microarray data from this study are available through the National Center for Biotechnology Information Gene Expression Omnibus database under accession number GSE65412.

RESULTS

Innate immune gene expression profiles induced by NYVAC-C vaccine vectors in primary human monocytes. The gene expression profiles induced by NYVAC-C, NYVAC-C-ΔB19R, and NYVAC-C-ΔB8RB19R in human primary monocytes 6 h after infection were analyzed by use of a microarray. Relative to the transcription profile of mock-infected monocytes, NYVAC-C and NYVAC-C-ΔB19R induced the expression of 2,437 genes in common (fold change, >1.3; $P < 0.05$), while 1,757 and 110 genes were differentially regulated uniquely by NYVAC-C and by NYVAC-C-ΔB19R, respectively (Fig. 1A; see also Table S3 in the supplemental material). Comparison of NYVAC-C and NYVAC-C-ΔB8RB19R revealed that they altered the expression of 3,429 common genes, while the expression of 765 and 342 genes was induced uniquely by NYVAC-C and by NYVAC-C-ΔB8RB19R, respectively (Fig. 1C; see also Table S4 in the supplemental material). Relative to the genes whose expression was induced by NYVAC-C, NYVAC-C-ΔB19R and NYVAC-C-ΔB8RB19R induced the expression of 25 common genes, whereas 570 and 5 genes were induced uniquely by NYVAC-C-ΔB19R and NYVAC-C-ΔB8RB19R, respectively (Fig. 1E; see also Table S5 in the supplemental material). These results demonstrate that NYVAC-C-ΔB8RB19R shares a significantly higher number of differentially induced genes with NYVAC-C than with NYVAC-C-ΔB19R.

We then compared the transcription profiles of monocytes infected with NYVAC-C, NYVAC-C-ΔB19R, or NYVAC-C-ΔB8RB19R using fold change scatter plots, as depicted in Fig. 1D to F. Genes falling on the identity line were expressed at similar levels by both vectors in primary monocytes. Both NYVAC-C-ΔB19R and NYVAC-C-ΔB8RB19R induced a gene expression signature that was highly correlated to that induced by NYVAC-C ($r = 0.93$ for NYVAC-C-ΔB19R, $r = 0.96$ for NYVAC-C-ΔB8RB19R) (Fig. 1B and D). Comparison of the gene expression signatures induced by NYVAC-C-ΔB19R and NYVAC-C-ΔB8RB19R relative to the signature induced by NYVAC-C showed that the overlap in gene expression was significantly lower

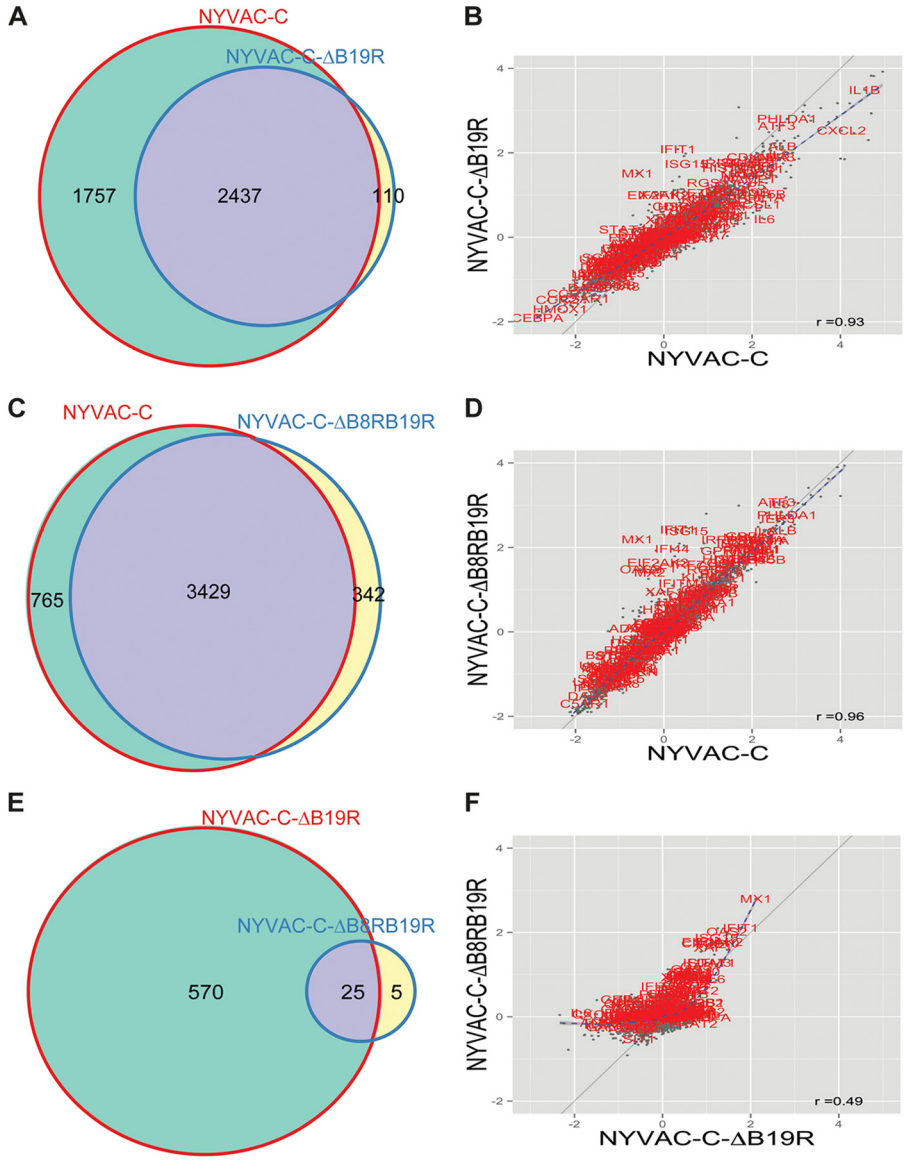

FIG 1 Venn diagrams and scatter plots of fold changes in expression of genes differentially induced by NYVAC-C, NYVAC-C-ΔB19R, and NYVAC-C-ΔB8RB19R in human monocytes. Venn diagrams (A, C, and E) depicting the number of genes differentially induced (fold change, >1.3; adjusted *P* value, <0.1) and scatter plots (B, D, and F) depicting fold changes in gene expression in human primary monocytes infected for 6 h with NYVAC-C, NYVAC-C-ΔB19R, or NYVAC-C-ΔB8RB19R (MOI, 5) relative to the levels of gene expression in control cells consisting of either mock-infected monocytes or monocytes infected with NYVAC-C. (A and B) Gene expression in NYVAC-C- versus NYVAC-C-ΔB19R-infected cells (MOI, 5) relative to that in mock-infected cell cultures; (C and D) gene expression in NYVAC-C-ΔB19R- versus NYVAC-C-ΔB8RB19R-infected cells (MOI, 5) relative to that in mock-infected cell cultures; (E and F) gene expression in NYVAC-C-ΔB19R- versus NYVAC-C-ΔB8RB19R-infected cells (MOI, 5) relative to that in NYVAC-C-infected cells. In the fold change scatter plots, the genes falling on the identity line (dark gray line) exhibited similar levels of expression in both systems. A loess curve (dashed blue line) was used to infer the local trend between the two systems. IFN-dependent genes differentially expressed in at least one comparison are highlighted in red. Solid lines indicate absolute 2-fold changes. The *x* and *y* axes in the scatter plots show the $\log_2$(FC) in the level of gene expression after 6 h of stimulation with NYVAC-C, NYVAC-C-ΔB19R, or NYVAC-C-ΔB8RB19R.

($r = 0.49$) than that when the gene expression signatures induced by NYVAC-C-ΔB19R and NYVAC-C-ΔB8RB19R were compared to the gene expression signature for mock-infected cells (Fig. 1F). Figure 1B shows genes whose expression was induced by NYVAC-C and NYVAC-C-ΔB19R relative to those whose expression was induced in mock-infected cells, with IFN-dependent genes being highlighted in red. The genes induced by NYVAC-C-ΔB19R included those for antiviral effector molecules, mostly IFN-stimulated genes (ISGs), such as genes for IFIT1, IFIT2, IFIT3, ISG15, MX1, MX2, IFI44, IFIT44L, STAT1, OAS2, CXCL10, IFITM3, and the transcription factor IRF9. While NYVAC-C did not induce any ISGs, it triggered the expression of several proinflammatory cytokines (IL-1A, IL-1B, IL-6, IL-8, TNF, tumor necrosis factor receptor superfamily 4 [TNFRSF4]) and chemokines (CXCL1, CCL20, CXCL2) that were not induced by NYVAC-C-ΔB19R (a full list of genes is provided in Table S6 in the supplemental material).

Comparative analysis of the genes induced by NYVAC-C and

NYVAC-C-ΔB8RB19R relative to the genes induced in mock-infected cells indicated that while both vectors induced the expression of a highly overlapping set of genes, including those for proinflammatory cytokines (IL-1A, IL-1B, IL-6, IL-8, TNF), only NYVAC-C-ΔB8RB19R induced the expression of several ISGs, including MX1, MX2, OAS2, IFI6, IFIT1, IFIT2, IFIT3, ISG15, IFI44, and IFI44L (Fig. 1D; see also Table S7 in the supplemental material). Finally, scatter plot analysis of the genes induced by NYVAC-C-ΔB19R and NYVAC-C-ΔB8RB19R relative to those induced by NYVAC-C confirmed that although NYVAC-C-ΔB19R and NYVAC-C-ΔB8RB19R shared the upregulation of many ISGs, their global gene expression profiles remained very distinct ($r = 0.43$) (Fig. 1F), as illustrated in the Venn diagram in Fig. 1E (see also Table S8 in the supplemental material).

To validate the gene expression findings, we next quantified with the OpenArray real-time PCR platform the expression of 112 genes (see Table S2 in the supplemental material) selected from among those involved in various signaling pathways in monocytes stimulated with NYVAC-C, NYVAC-C-ΔB19R, or NYVAC-C-ΔB8RB19R (Fig. 2). The OpenArray data confirmed the expression trends for most of the genes, as shown by the overall agreement between the fold change in the levels of gene expression induced by NYVAC-C ($r = 0.48$; Fig. 2A), NYVAC-C-ΔB19R ($r = 0.65$; Fig. 2B), and NYVAC-C-ΔB8RB19R ($r = 0.52$; Fig. 2C) in human monocytes relative to the levels of expression in mock-infected monocytes obtained from the Illumina microarrays and from the OpenArray real-time PCR. Overall, these data highlight the fact that while both NYVAC-C-ΔB19R and NYVAC-C-ΔB8RB19R induced the expression of type I and type II IFNs and IFN-inducible genes, only NYVAC-CΔB8RB19R was capable of inducing the activation of proinflammatory cytokines.

Pathway analysis reveals distinct innate immune responses induced by NYVAC-C-ΔB19R and by NYVAC-C-ΔB8RB19R. We next defined the molecular and functional pathways induced by the different NYVAC mutants and compared the patterns of pathway enrichment observed 6 h after infection in human primary monocytes. Enrichment was performed using the list of genes differentially expressed after NYVAC-C-ΔB8RB19R infection, which was compared to the list of genes induced by NYVAC-C-ΔB19R (Fig. 3). A full list of genes is provided in Table S8 in the supplemental material. Compared to the genes induced by NYVAC-C-ΔB19R, NYVAC-C-ΔB8RB19R induced the coordinate upregulation of several innate immune response pathways, including TREM1 signaling, dendritic cell maturation, IL-8 signaling, cross talk between dendritic cells and NK cells, and NF-κB signaling. These pathways comprised several antiviral molecules (MX1, OAS2, IFIT3, IFITM1) and proinflammatory cytokines (IL-6, IL-8, TNF) and chemokines (CCL3) of the innate immune response. Interestingly, the inflammasome pathway was also activated by NYVAC-C-ΔB8RB19R, as illustrated by the upregulation of genes belonging to the inflammasome molecular signature (IL-1A, IL-1B, and CASP1) (Fig. 3). The pathway regulating the cross talk between innate and adaptive immune cells was further identified to be a molecular signature induced by NYVAC-C-ΔB8RB19R, with the expression of cell surface receptors that enhance T cell activation, such as CD40 (binding CD40L), CD86, CD58 (ligand for the T cell costimulatory molecule CD2), and HLA-DMA and HLA-DMB (both of which are involved in antigen presentation by major histocompatibility complex class II molecules) (Fig. 3). Transcription factors and critical intermediates of the NF-κB signaling pathway (namely, NF-κB1, RELB, TRAF1, TBK1, and TANK) or of the JAK-STAT pathway downstream of cytokine receptors (STAT4), all of which positively regulate inflammation, were also induced by NYVAC-C-ΔB8RB19R. Finally, NYVAC-C-ΔB8RB19R induced the expression of CD83, suggesting that this vector could promote the maturation of monocytes to dendritic cells through the upregulation of CD83 and proinflammatory cytokines (29). Altogether, these data demonstrate that the deletion of type I and type II IFN-binding molecules from NYVAC-C led not only to the restoration of IFN signaling pathways but also to the activation of various innate immune pathways that should contribute to a strong adaptive immune response.

Differential expression of type I and type II IFN-stimulated genes in monocytes infected with NYVAC-C-ΔB19R or NYVAC-C-ΔB8RB19R. Given the importance of type I and type II IFNs in the antiviral response and the significant induction of genes belonging to the IFN signaling pathways and of ISGs in the gene array profiling, we next performed a gene expression heat map of ISGs differentially expressed by primary monocytes infected with NYVAC-C, NYVAC-C-ΔB19R, or NYVAC-C-ΔB8RB19R relative to their expression in mock-infected monocytes (Fig. 4A to C). To do this, we applied type I (IFN-α) and type II (IFN-γ) filters to determine the IFN responses that were either unique to or shared between NYVAC-C, NYVAC-C-ΔB19R, and NYVAC-C-ΔB8RB19R with the specific aim to correlate the IFN-related mutations of the vectors with a specific IFN response.

By applying a type I (IFN-α) filter, we observed that the results for NYVAC-C-ΔB19R and NYVAC-C-ΔB8RB19R clustered together, inducing the increased expression of type I IFN-dependent genes known to exhibit antiviral functions (IRF7, ISG15, ISG20, IFIT1, IFI44, IFITM1, EIF2AK2, MX1, MX2, OAS1, OAS2, STAT2) (Fig. 4A). Interestingly, induction of expression of a small cluster of IFN-α-filtered genes was not shared by NYVAC-C-ΔB19R and NYVAC-C-ΔB8RB19R but was common to NYVAC-C and NYVAC-C-ΔB8RB19R. This cluster mostly comprised proinflammatory genes (such as IL-6 and PLAU) and DUSP5, which are considered to be involved in the type I IFN-associated acute-phase response and suggested that there were two different IFN signatures induced by NYVAC-C-ΔB19R and NYVAC-C-ΔB8RB19R.

The second IFN signature was better delineated after applying an IFN-γ filter (Fig. 4B). Indeed, the clustering of IFN-γ-related genes led to a clustering different from that observed with the IFN-α filter. NYVAC-C-ΔB19R and NYVAC-C-ΔB8RB19R clustered together through the coordinated expression of IFN-γ-related or associated genes, such as IRF1 and IRF8, as well as proinflammatory mediators (IL-1A, IL-1B, and TNFAIP2), effector molecules (GBP1, GBP2, and GADD45B), and an adhesion molecule (ICAM-1) (Fig. 4B). Of note, CXCL10, a proinflammatory IFN-mediated chemokine with a dual function in regulating both innate and adaptive immunity, did not belong to this cluster and was also induced by both NYVAC-C and NYVAC-C-ΔB8RB19R (30). Finally, we determined the expression of genes induced by NYVAC-C, NYVAC-C-ΔB19R, and NYVAC-C-ΔB8RB19R after both IFN-α and IFN-γ filtering (Fig. 4C). Again, NYVAC-C-ΔB19R and NYVAC-C-ΔB8RB19R clustered together, given their high levels of induction of type I IFN-dependent genes. Confirming our earlier results, proinflammatory genes, such as CCL8 and TNFSF10, were induced by both NYVAC-C-ΔB19R and NYVAC-

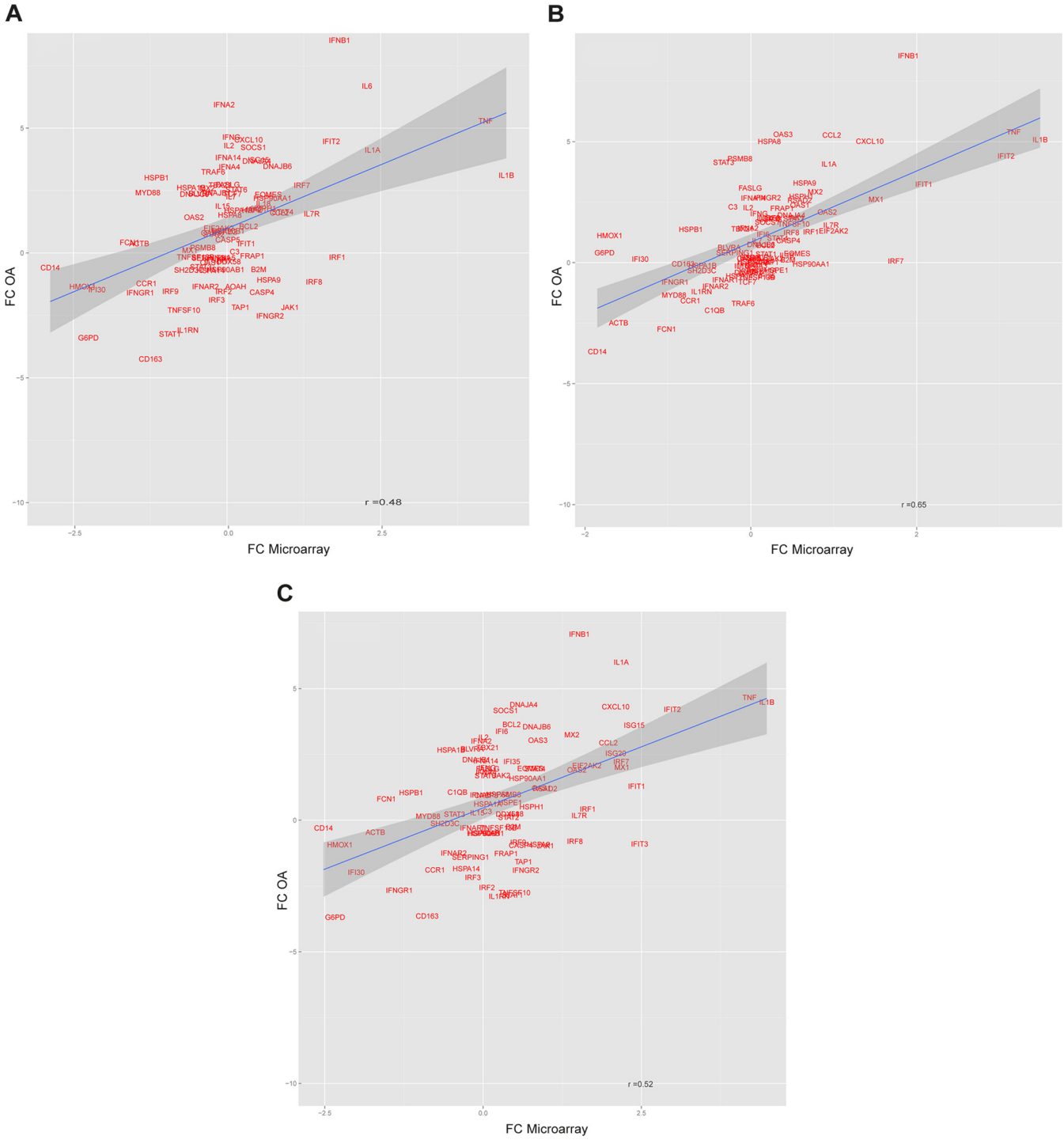

FIG 2 Gene expression values from the Illumina BeadArrays plotted against the OpenArray real-time PCR $-\Delta C_T$ values for each target gene. Scatter plots comparing the fold change in gene expression between the Illumina microarrays and OpenArray real-time PCR (OA) in human primary monocytes infected for 6 h with NYVAC-C (A), NYVAC-C-ΔB19R (B), and NYVAC-C-ΔB8RB19R (C) relative to the levels of expression in mock-infected cells are shown. PCR targets were mapped to the BeadArray probes by matching the official gene symbols. The correlations indicated are the sample Pearson correlation coefficients.

C-ΔB8RB19R, whereas CASP1 was induced by both NYVAC-C and NYVAC-C-ΔB8RB19R but not by NYVAC-C-ΔB19R (Fig. 4C). Overall, these results demonstrate that both NYVAC-C-ΔB19R and NYVAC-C-ΔB8RB19R triggered a robust type I IFN gene response, but only NYVAC-C-ΔB8RB19R was capable of inducing the expression of cytokines, notably, cytokines associated with the inflammasome pathway.

Network analysis shows differential induction of IFNs and pro-inflammatory pathways in monocytes infected with NYVAC-C-ΔB19R and NYVAC-C-ΔB8RB19R. We next performed network

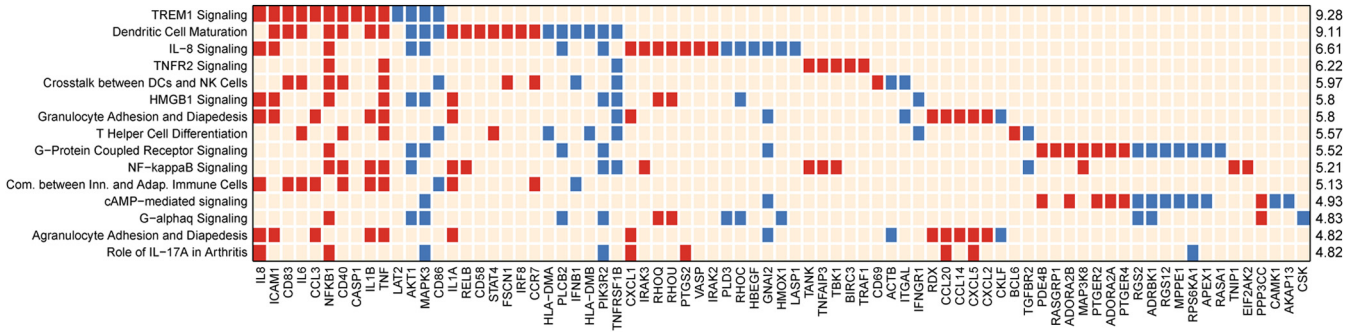

FIG 3 Comparison of the patterns of pathway enrichment in monocytes infected with NYVAC-C-ΔB8RB19R and monocytes infected with NYVAC-C-ΔB19R. The pathways and genes induced in human primary monocytes infected for 6 h with NYVAC-C-ΔB8RB19R relative to those induced in human primary monocytes infected with NYVAC-C-ΔB19R are shown. Each row is an upregulated canonical innate immune pathway (Ingenuity software); each column represents an upregulated (red) or downregulated (blue) gene involved in one or more regulated pathways. The overrepresentation test was performed using Fisher's exact test, and the statistical significance, displayed on the right *y* axis, was achieved for *P* values of <0.05 [$-\log(P) > 1.3$]. TNFR2, TNF receptor 2; DCs, dendritic cells; Com., communication; Inn., innate; Adap., adaptive; cAMP, cyclic AMP; G-alphaq signaling, G protein-alphaq signaling.

inference analysis of the genes and canonical pathways induced by the different poxvirus vectors to confirm the coordinated interaction between these genes in immunologically relevant biological pathways (Fig. 5). Top network analysis showed that proinflammatory cytokines, such as TNF, were downregulated by NYVAC-C-ΔB19R compared to the level of expression after infection with NYVAC-C (Fig. 5A). The downregulation of TNF was correlated to the downregulation of the NF-κB transcriptional network (NF-κB1, NF-κB2, IκB, RELA, RELB) and the signal transduction machinery that regulates these transcription factors (TANK, TBK1, TRAF2) (Fig. 5B and data not shown). The decreased expression of these transcription factors most likely resulted in the downregulation of several proinflammatory cytokines, including IL-1 and IL-6 (Fig. 5A and B). Cell surface molecules (TNFRSF18/GITR, TNFRSF10B/TRAIL) of ligands or receptors that control T cell activation were also downregulated upon infection of monocytes with NYVAC-C-ΔB19R (data not shown). Interestingly, KMO, which negatively regulates NF-κB-induced inflammation, was downregulated by NYVAC-C-ΔB19R (Fig. 5A). This feedback loop is not supposed to be required, since the levels of expression of both TNF and NF-κB were decreased after NYVAC-C-ΔB19R infection (Fig. 5A). Network analysis of genes upregulated by NYVAC-C-ΔB8RB19R compared to their levels of expression after infection with NYVAC-C confirmed the importance of type I IFNs with IRF7, a master regulator gene of the type I interferon pathway, which is the central node of this network (Fig. 5C). As expected, increased levels of IRF7 resulted in the upregulation of several antiviral ISGs (MX1, ISG15, OAS2, IFIT1, IFIT2, IFIT3, IFI44) as well as chemokines (data not shown) typical of the primary antiviral response. We also observed an upregulation of X-linked inhibitor of apoptosis (XIAP)-associated factor 1 (XAF1), a gene downstream of the genes for type I IFNs and TNF in cells infected with NYVAC-C-ΔB8RB19R (Fig. 5C) (31). XAF-1 inhibits XIAPs, thereby promoting apoptosis of infected cells and, potentially, cross priming (Fig. 5C) (32). Direct comparison of NYVAC-C-ΔB8RB19R and NYVAC-C-ΔB19R further highlighted their differences (Fig. 5D and E). The top two networks that received a high score by IPA confirmed that NYVAC-C-ΔB8RB19R upregulated IFN-dependent genes (Fig. 5E), TNF, and downstream targets, such as IL-1 and IL-6, compared to their levels of expression in cells infected with NYVAC-C-ΔB19R (Fig. 5D). Thus, as was observed in Fig. 1, NYVAC-C-ΔB19R and NYVAC-C-ΔB8RB19R exerted very distinct effects on transcriptional and signal transduction networks. NYVAC-C-ΔB19R induced only type I IFN responses, while NYVAC-C-ΔB8RB19R induced a more complex response that integrated type I IFNs, inflammatory cytokines, and the inflammasome signaling pathways.

NYVAC-C-ΔB8RB19R induces the robust production of proinflammatory mediators in primary monocytes and activates IRF and STAT1 signaling pathways. To further validate the microarray profiling and RT-PCR data, we next measured the production of proinflammatory cytokines, chemokines, and type I IFNs in primary monocytes infected for 24 h with NYVAC-C, NYVAC-C-ΔB19R, or NYVAC-C-ΔB8RB19R. Consistent with our previous observations (21), primary human monocytes infected with NYVAC-C-ΔB19R or NYVAC-C-ΔB8RB19R produced higher levels of IFN-α, IFN-β, and IP-10 than primary human monocytes infected with NYVAC-C (Fig. 6). Interestingly, NYVAC-C-ΔB8RB19R was a more potent inducer of type I IFNs, TNF, IL-1β, IL-6, and IL-8 than NYVAC-C and NYVAC-C-ΔB19R (Fig. 6). Sensing of NYVAC by macrophages relies on TLR2-TLR6-MyD88 and MDA-5–IPS-1, which play critical roles in the production of IFN-β and IFN-β-dependent chemokines (21).

Given that NYVAC-C-ΔB8RB19R stimulated powerful type I IFN and chemokine gene expression, we analyzed in more detail the signal transduction pathways and transcription factors implicated in the production of these mediators in THP-1 cells. We focused on phospho-IRF3 (P-IRF3), which is essential for transcription of the *IFNB* gene, and IRF7 and phospho-STAT1 (P-STAT1), which are critical for the transcriptional activation of IFN-β-dependent genes. In line with our previous observations, NYVAC-C induced only a very weak induction of P-IRF3, IRF7, and P-STAT1. In contrast, NYVAC-C-ΔB19R and NYVAC-C-ΔB8RB19R induced much stronger P-IRF3, IRF7, and P-STAT1 signals than NYVAC-C (Fig. 7). Thus, NYVAC-C-ΔB8RB19R induced robust intracellular signaling (i.e., signaling of NF-κB, IRF3, IRF7, and STAT1) in the human THP-1 monocytic cell line.

These results confirm that NYVAC-C-ΔB19R and NYVAC-C-ΔB8RB19R induce more powerful type I IFN and IFN-dependent chemokine production than NYVAC-C. Moreover, NYVAC-C-ΔB8RB19R was the only poxvirus vector capable of inducing a

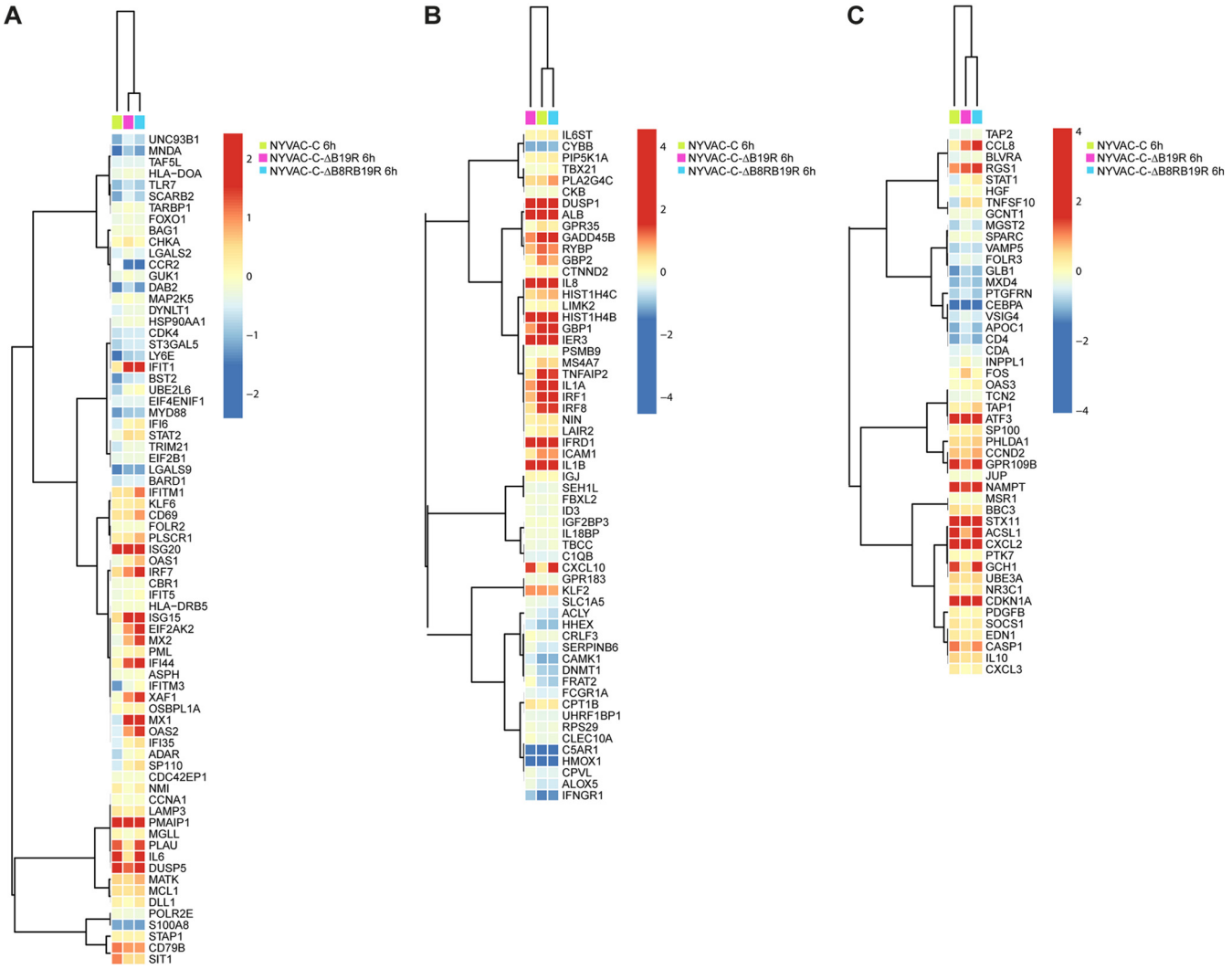

FIG 4 Heat map of IFN-filtered genes differentially expressed in human monocytes infected with NYVAC-C, NYVAC-C-ΔB19R, or NYVAC-C-ΔB8RB19R. Human primary monocytes were infected for 6 h with NYVAC-C, NYVAC-C-ΔB19R, or NYVAC-C-ΔB8RB19R (MOI, 5). The heat map depicts differential ISG expression, reported as the average fold change in gene expression relative to the levels of expression in mock-infected monocytes. The genes were immune filtered using three lists of IFN genes: IFN-α genes (A), IFN-γ genes (B), and genes common to both IFN-α and IFN-γ (C). The genes selected are the top genes significantly expressed in at least one contrast following an analysis of variance *F* test and selected to be differentially expressed on a fold change basis of up- or downregulation of 1.3-fold and an adjusted *P* value of <0.1. The color legend indicates fold changes over the levels of expression in mock-infected cells, and the fold changes are expressed on a $\log_2$ scale, where red and blue correspond to up- and downregulation, respectively.

vigorous proinflammatory cytokine response, characterized by the release of high levels of TNF, IL-1β, IL-6, and IL-8.

Type I IFNs are key modulators of the increased immunogenicity induced by NYVAC-C-ΔB8RB19R. To confirm the hypothesis that the improved immunogenic profile of NYVAC-C-ΔB8RB19R was mediated by type I IFNs, human THP-1 cells were pretreated with anti-IFN-α and anti-IFN-β antibodies 1 h prior to infection with NYVAC-C, NYVAC-C-ΔB19R, or NYVAC-C-ΔB8RB19. Gene expression was analyzed at 3 h postinfection. Neutralization of IFN-α/β resulted in a statistically significant reduction in the levels of expression of ISGs (*IFIT1*, *IFIT2*), IFN-dependent chemokines (CXCL10/IP-10), and type III IFN (IL-29) to levels close to those triggered by NYVAC-C (Fig. 8A). The levels of transcription factors implicated either in the regulation of IFN transcription (IRF7) or in IFN signaling pathways (STAT1) were also reduced following IFN-α/β blockade (Fig. 8A). Moreover, when IFN-α/β was blocked, a significant decrease in the production of IFN-β and CXCL10/IP-10 was observed in human THP-1 cells infected with NYVAC-C-ΔB19R and NYVAC-C-ΔB8RB19R (Fig. 8B). Overall, these results argue in favor of a critical role for type I IFNs as master regulators of multiple aspects of the innate immune response induced by NYVAC-C-ΔB19R and NYVAC-C-ΔB8RB19.

Monocytes infected with NYVAC-C-ΔB8RB19R induce a strong proliferation of allogeneic $CD4^+$ T cells. We next investigated whether the improved innate immune responses induced by the deletion mutants compared with those induced by the parental NYVAC-C vaccine vectors translated into improved adaptive immune responses. This question was examined using a classical T cell proliferation assay in which human monocytes were

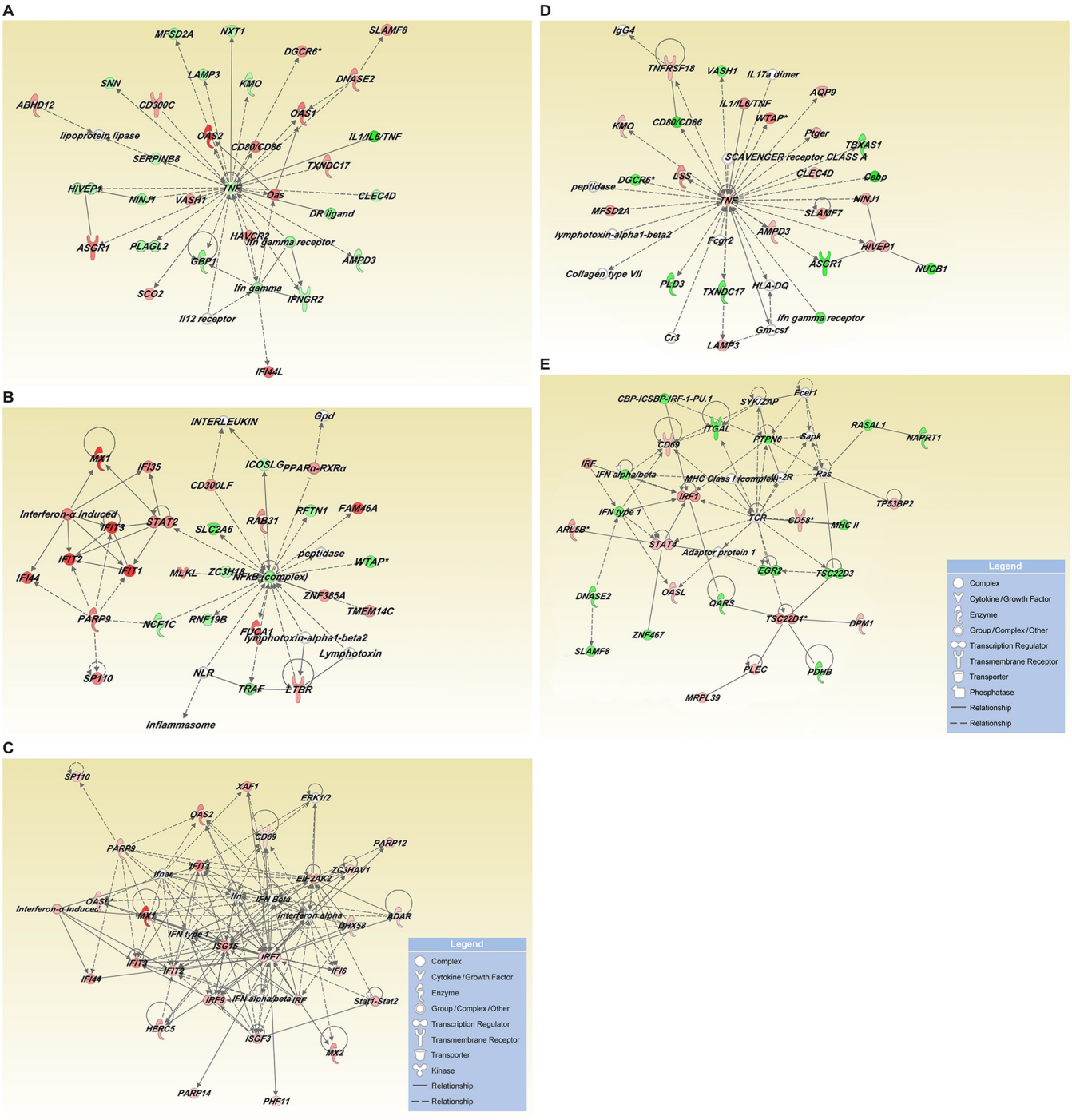

FIG 5 Gene interaction networks differentially induced with NYVAC-C-ΔB19R and NYVAC-C-ΔB8RB19R in human monocytes. Human primary monocytes were infected for 6 h with NYVAC-C, NYVAC-C-ΔB19R, or NYVAC-C-ΔB8RB19R (MOI, 5). Gene interaction networks were built on the basis of genes differentially induced by NYVAC-C-ΔB19R (A, B) and NYVAC-C-ΔB8RB19R (C) relative to their levels of expression in cells infected with NYVAC-C or differentially induced by NYVAC-C-ΔB8RB19R relative to their levels of expression in cells infected with NYVAC-C-ΔB19R (D, E) by using the Ingenuity Pathways Knowledge Base (IPKB). Genes are highlighted in red (upregulation) or green (downregulation), and node properties are indicated by shape, as indicated in the legends. Interactions between the different nodes are given as solid (direct interaction) and dashed (indirect interaction) lines (edges), with various colors used for the different interaction types. The networks are the results of merging of the top two networks that received a high score by IPA.

infected for 18 h with NYVAC-C, NYVAC-C-ΔB19R, or NYVAC-C-ΔB8RB19R and then cocultured for 5 days with allogeneic $CD4^+$ T cells. As shown in Fig. 9A, monocytes infected with NYVAC-C-ΔB8RB19R induced the stronger proliferation of naive $CD4^+$ T cells than monocytes infected with NYVAC-C and NYVAC-C-ΔB19R. Interestingly, the concentrations of IFN-α and IFN-β produced by monocytes after poxvirus infection correlated with the proliferation of $CD4^+$ T cells (data not shown).

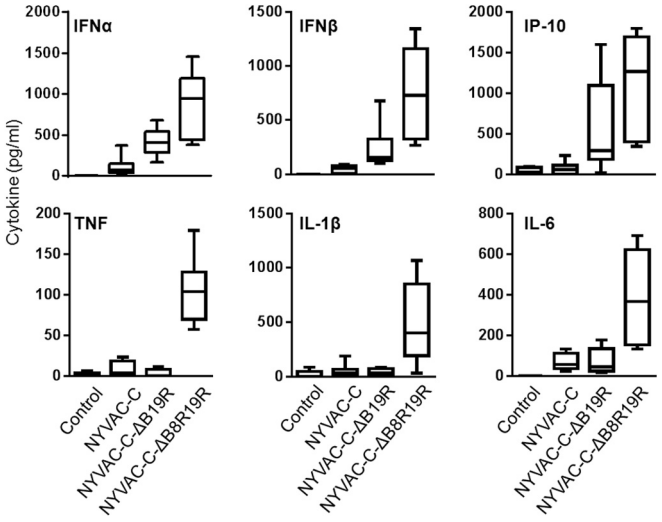

FIG 6 Type I interferons, cytokines, and chemokines released by human monocytes infected with NYVAC-C, NYVAC-C-ΔB19R, and NYVAC-C-ΔB8RB19R. Monocytes from healthy volunteers were infected for 24 h with NYVAC-C, NYVAC-ΔB19R, or NYVAC-CΔB8RB19R, and the concentrations of IFN-α, IFN-β, CXCL10/IP-10, TNF, IL-1β, and IL-6 were measured in cell culture supernatants. Box plots of three separate experiments including a total of eight subjects are shown. Data points are means for duplicate or triplicate samples per subject. Bottom, median, and top lines, 25th, 50th, and 75th percentiles, respectively; vertical lines with whiskers, the range of values.

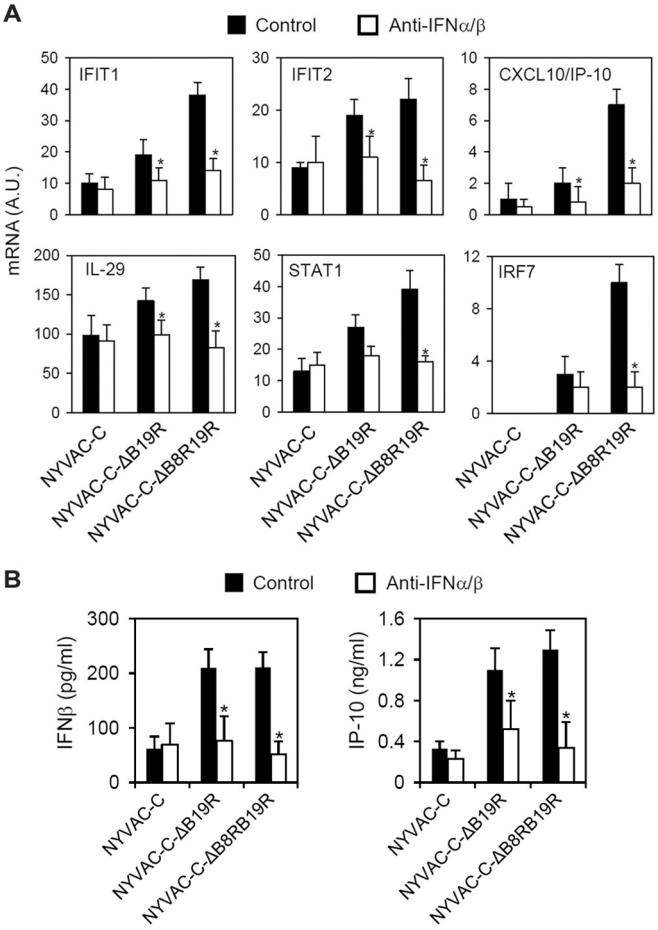

FIG 8 Expression of chemokines and transcription factors induced by NYVAC-C-ΔB8RB19R in human monocytic cells is type I IFN dependent. Human THP-1 monocytic cells were preincubated for 1 h with control or anti-IFN-α/β antibody (10 μg/ml) and then stimulated for 3 h with NYVAC-C, NYVAC-C-ΔB19R, and NYVAC-C-ΔB8RB19R (MOI, 5). (A) Gene expression levels were analyzed by RT-PCR, and the results are expressed as the ratio of gene to HPRT mRNA levels. A.U., arbitrary units. (B) Cell-free supernatants were collected after 24 h to quantify the concentrations of IFN-β and CXCL10/IP-10. Data are means ± SDs for triplicate samples from one experiment and are representative of those from three independent experiments. *, $P < 0.05$ for anti-IFN-α/β versus control antibody.

This led us to determine whether the increased proliferation was driven by type I IFNs. Human monocytes were pretreated with an anti-IFN-α and anti-IFN-β antibody before exposure to NYVAC-C, NYVAC-C-ΔB8RB19R, or NYVAC-C-ΔB8RB19R and were then cocultured with allogeneic naive $CD4^+$ T cells for 5 days. As shown in Fig. 9B, blockage of IFN-α/β markedly reduced the rate of proliferation of $CD4^+$ T cells cocultured with NYVAC-C-ΔB19R- or NYVAC-C-ΔB8RB19R-infected monocytes.

The microarray data revealed an enhanced expression of the inflammasome pathways in human monocytes infected by NYVAC-C-ΔB8RB19R. Given the roles played by NOD-like receptors (NLRs) and the inflammasomes in the host antiviral defense response (33), we sought to determine whether the increased proliferation rate could also be dependent upon IL-1β production. As shown in Fig. 9C, blockage of IL-1β activity with IL-1ra, an antagonist of the type I IL-1 receptor, markedly reduced the rate of proliferation of $CD4^+$ T cells cocultured with monocytes infected with NYVAC-C-ΔB8RB19R, suggesting that activation of the inflammasome leading to IL-1β played an active role in the enhanced immunogenic profile of NYVAC-C-ΔB8RB19R. Collectively, these results showed that monocytes infected with NYVAC-C-ΔB8RB19R induce a strong proliferative $CD4^+$ T cell response in a type I IFN- and IL-1-dependent manner.

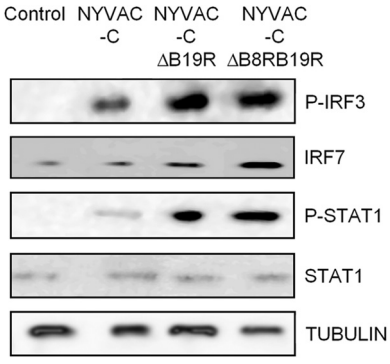

FIG 7 NYVAC-C-ΔB19R and NYVAC-C-ΔB8RB19R activate IRF3, IRF7, and STAT1 transcription factors. Cytosolic extracts were obtained from THP-1 cells infected for 6 h with NYVAC-C, NYVAC-C-ΔB19R, or NYVAC-C-ΔB8RB19R (MOI, 5). The expression of P-IRF3, IRF7, P-STAT1, STAT1, and tubulin was analyzed by Western blotting. Results are representative of those from three independent experiments.

DISCUSSION

Deletion of a single gene (*B19R*) or two genes (*B8R* and *B19R*) encoding proteins acting as antagonists of type I and type II IFN-mediated antiviral host defenses resulted in a striking enhancement of the immunogenic properties of a NYVAC vaccine vector. Systems biology analyses revealed that deletion of *B19R*, a type I IFN-binding protein, resulted in markedly enhanced innate im-

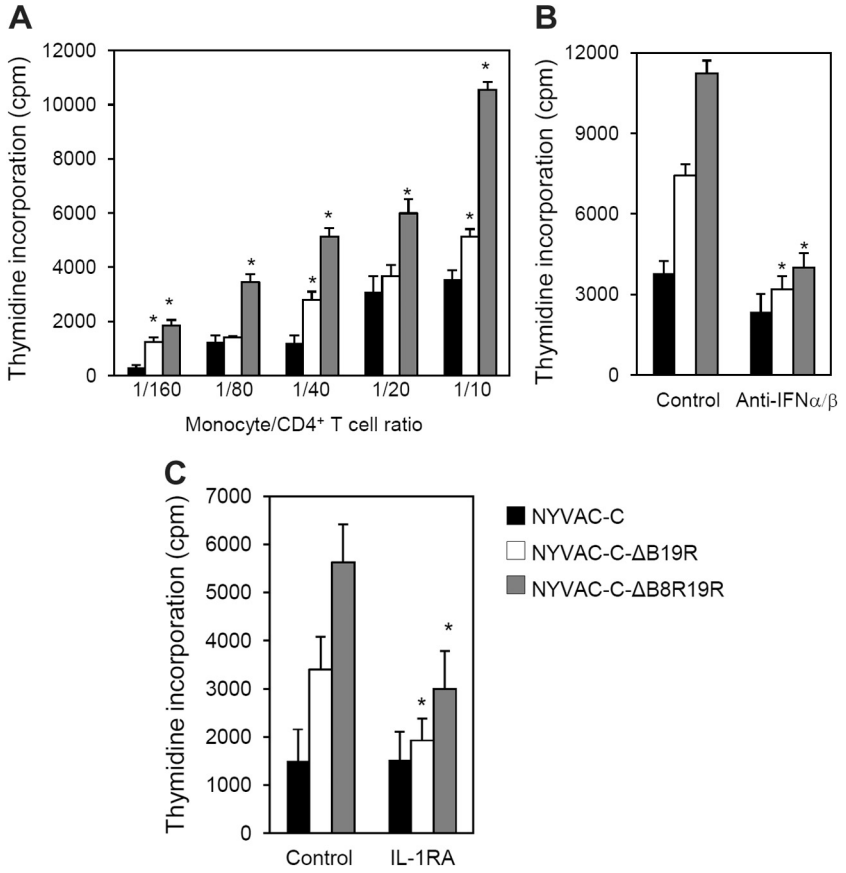

FIG 9 Type 1 IFN- and IL-1-dependent induction of allogeneic $CD4^+$ T cell response by primary monocytes infected with NYVAC-C-ΔB8RB19R. Primary human monocytes were infected for 18 h with NYVAC-C, NYVAC-C-ΔB19R, or NYVAC-C-ΔB8RB19R (MOI, 1) in the absence (A) or in the presence (B, C) of control, anti-IFN-α/β (B), or IL-1ra (C) antibody (10 μg/ml). Monocytes were collected, washed, and added to $CD4^+$ T cells at monocyte/$CD4^+$ T cell ratios ranging from 1/10 to 1/160 (A) or at a fixed 1/10 ratio (B, C). After 5 days, T cell proliferation was analyzed by measurement of the level of thymidine incorporation. Data are means ± SDs for triplicate samples from one experiment and are representative of those from two separate experiments. *, $P < 0.05$ for mutant versus wild-type NYVAC-C.

mune responses of monocytes, characterized by the upregulated expression of IRF7 and STAT1 and the robust production of type I IFNs and of ISGs whose expression was inhibited by anti-type I IFN antibodies. Infection of monocytes with an NYVAC vector with combined deletion of type I and type II IFN-binding proteins (NYVAC-C-ΔB8RB19R) resulted in higher levels of expression of IRF7 and STAT1, more type I IFN production, and the much broader upregulation of ISGs. Furthermore, in sharp contrast to the findings for the single deletion mutant, the double deletion mutant also induced a prominent proinflammatory cytokine response (TNF, IL-6, and IL-8) and strong activation of canonical inflammasomes (caspase-1 and IL-1β).

Type I IFNs may be induced in an autocrine manner via a feed-forward loop mediated by proinflammatory cytokines, such as TNF, which have been shown to be strongly upregulated by NYVAC-C-ΔB8RB19R (34, 35). Indeed, the burst of proinflammatory cytokines was a striking characteristic of the immune profile induced by the double mutant, underscored by the critical role played by NF-κB signaling and TNF as the top two gene expression nodes identified by network interference analyses. Until now, the B19 and B8 poxvirus proteins were considered to act as soluble decoy IFN receptors interfering with the binding of type I and type II IFNs to their cognate receptors (36–42). Alternatively, the present findings may indicate that the B19 and B8 poxvirus proteins exhibit other IFN-modulating properties. The fact that the expression of IFN-α and IFN-β was markedly upregulated upon infection of monocytes with NYVAC-C-ΔB19R and NYVAC-C-ΔB8RB19R suggests that the B19 and B8 proteins also interfere with innate immune sensing of poxviruses or downstream signal transduction pathways leading to the production of type I IFNs. Indeed, IRF3 and IRF7, two critical transcription factors regulating the expression of type I IFNs, were found to be strongly upregulated by cells infected with NYVAC-C-ΔB19R and NYVAC-C-ΔB8RB19R. Neither the single nor the double mutant impacted the levels of pattern recognition receptors implicated in the sensing of NYVAC, such as TLRs, RIG-I, and MDA5 (21, 42). Of note, all experiments were performed with human macrophages. We therefore do not know whether these observations also pertain to additional targets of poxviruses, such as other antigen-presenting cells (i.e., dendritic cells or B cells) or to activated T cells, yet, consistent with our findings, Quakkelaar et al. reported that deletion of the gene for the B19R protein in NYVAC-C enhanced type I IFN production and the expression of ISGs in conventional and plasmacytoid dendritic cells (43).

Another salient feature of the immunogenicity stimulated by NYVAC-C-ΔB8RB19R in monocytes was the upregulation of a

canonical inflammasome response with the production of high levels of caspase-1 and IL-1β. The NLRP1, NLRP3, NLRC4, AIM2, and RIG-I/MDA5 inflammasomes have been implicated in numerous host antiviral defensive responses (21, 44–48). With respect to poxviruses we have shown previously that MVA and NYVAC activate the NLRP3 inflammasome (21). Other investigators have also demonstrated a role for the NLRP3 and AIM2 inflammasomes in the recognition of encephalomyocarditis virus 16 and vaccinia virus, respectively (48, 49). The presence of multiple inhibitors of ASC, caspase-1, IL-1β, or IL-18, including homologues of serpin-like protease inhibitors like SPI-2/CrmA or Serp2 targeting caspase-1, in the genome of poxviruses emphasizes the importance of the inflammasome pathway in antiviral immunity (50, 51).

The differential expression of the inflammasome signature by NYVAC-C-ΔB19R and by NYVAC-C-ΔB8RB19R is explained at least in part by the opposite effects of the type I and type II IFNs at the level of the activation of inflammasomes. The downregulation of caspase-1 and IL-1β by NYVAC-C-ΔB19R was most likely caused by the enhanced production of type I IFNs, shown previously to inhibit IL-1β production in macrophages. This inhibition resulted in the repression of NLRP1 and NLRP3 expression by type I IFNs in, on the one hand, a STAT1-dependent manner and, on the other hand, via an autocrine, STAT3-dependent inhibitory effect of IL-10 (52). IFN-β has also been shown to suppress the activation of the NLRP3 inflammasome in macrophages via the successive engagement of SOCS-1, Vav1, and the Rho GTPase Rac 1 and the generation of reactive oxygen species (53). Moreover, IFI16, a type I IFN-inducible protein, suppressed caspase-1 activation by the NLRP3 and AIM2 inflammasomes in THP-1 monocytes (54), whereas the caspase-1 activity induced by vaccinia virus was restored when IFI16 was knocked down in endothelial cells (55). Our data also support the fact that the upregulation of caspase-1 and IL-1β in NYVAC-C-ΔB8RB19R-treated monocytes might be mediated by the counterregulatory effects of type II IFNs on the activity of inflammasomes. Indeed, IFN-γ enhanced the expression of caspase-1 and AIM2 in THP-1 cells (55). Although the role of type II IFNs in IL-1β regulation remains controversial, recent evidence suggests that it could promote IL-1β production by human cells (56). Given the important role played by the NF-κB pathway and TNF in the activation of NLRP3 inflammasomes (57, 58), part of the inflammasome-activating capacity of NYVAC-C-ΔB8RB19R may be due to its action on the NF-κB pathway and to the upregulation of TNF. Consistent with this hypothesis, activation of dendritic cells with vaccinia virus or double-stranded DNA induced the production of IL-1β via the successive activation of the DNA sensor Rad50, CARD9, and the NF-κB pathway (59).

Monocytes infected with NYVAC-C-ΔB8RB19R induced a stronger type I IFN-dependent and IL-1-dependent allogeneic $CD4^+$ T cell response than monocytes infected with NYVAC-C or NYVAC-C-ΔB19R, suggesting a potential synergism between IL-1β and type I IFNs in the regulation of the adaptive immune response induced by NYVAC. Interestingly, $CD4^+$ T cell activation by R848 has been shown to be mediated by the combination of type I IFNs and IL-1β in cocultures of dendritic cells and $CD4^+$ T cells (60). Moreover, synergistic interactions between IL-1β and type I IFNs limited virus replication in a West Nile virus infection model (61). Double deletion of the genes for B19R and B8R in NYVAC may thus affect a complex regulatory loop controlled by IFNs and IL-1β, resulting in an enhanced immunogenic profile. Of note, the improved immunogenicity revealed by use of the systems biology approach is well in line with the enhanced immunogenicity data (i.e., $CD8^+$ T cell-adaptive immune response) obtained in mice immunized with a DNA prime/NYVAC-C boost regimen using mutants with single or double B8R and B19R deletions in NYVAC-C expressing the HIV-1 Env, Gag, Pol, and Nef antigens (20, 22).

Type I IFNs play a crucial role in the host innate and adaptive immune responses against viruses. However, chronic type I IFN signaling has also been associated with disease progression in chronic viral infections caused by lymphocytic choriomeningitis virus (LCMV), simian immunodeficiency virus (SIV), or hepatitis C virus (HCV). In a mouse model of persistent LCMV infection, type I IFNs induced chronic immune activation, and blockage of the type I IFN receptor limited immune system activation and promoted the clearance of LCMV (62, 63). These dual properties of type I IFNs were also demonstrated in a rhesus macaque model of SIV infection. Administration of an antagonist of the type I IFN receptor at the onset of SIV infection enhanced the viral load and accelerated the loss of $CD4^+$ T cells, while treatment with IFN-α2a delayed the progression of infection. However, when given over a prolonged time during the chronic phase of SIV infection, IFN-α2a treatment was detrimental, promoting SIV infection and greater $CD4^+$ T cell depletion (64). At face value, these observations would suggest that the use of a poxvirus vaccine vector with an enhanced type I IFN- and cytokine-inducing profile, such as NYVAC-C-ΔB8RB19R, might be better in the acute than in the chronic phase of HIV disease.

In conclusion, dual deletion of type I and type II IFN immune evasion genes in NYVAC poxvirus generated a promising HIV vaccine vector candidate characterized by markedly enhanced innate and adaptive immunogenic properties that make it an attractive candidate HIV vaccine vector.

ACKNOWLEDGMENTS

This research was conducted as part of the Poxvirus T Cell Vaccine Discovery Consortium (PTVDC) and the RepliVax (a novel replication-competent flavivirus-based HIV vaccine platform as a priming component for improving the antibody response) consortia under the Collaboration for AIDS Vaccine Discovery with support from the Bill & Melinda Gates Foundation. Julie Delaloye is supported by a junior clinical scientist grant from the Leenaards Foundation.

REFERENCES

1. **Stephenson KE, Barouch DH.** 2013. A global approach to HIV-1 vaccine development. Immunol Rev **254:**295–304. http://dx.doi.org/10.1111/imr.12073.
2. **Klein F, Mouquet H, Dosenovic P, Scheid JF, Scharf L, Nussenzweig MC.** 2013. Antibodies in HIV-1 vaccine development and therapy. Science **341:**1199–1204. http://dx.doi.org/10.1126/science.1241144.
3. **Shiver JW, Fu TM, Chen L, Casimiro DR, Davies ME, Evans RK, Zhang ZQ, Simon AJ, Trigona WL, Dubey SA, Huang L, Harris VA, Long RS, Liang X, Handt L, Schleif WA, Zhu L, Freed DC, Persaud NV, Guan L, Punt KS, Tang A, Chen M, Wilson KA, Collins KB, Heidecker GJ, Fernandez VR, Perry HC, Joyce JG, Grimm KM, Cook JC, Keller PM, Kresock DS, Mach H, Troutman RD, Isopi LA, Williams DM, Xu Z, Bohannon KE, Volkin DB, Montefiori DC, Miura A, Krivulka GR, Lifton MA, Kuroda MJ, Schmitz JE, Letvin NL, Caulfield MJ, Bett AJ, Youil R, Kaslow DC, Emini EA.** 2002. Replication-incompetent adenoviral vaccine vector elicits effective anti-immunodeficiency-virus immunity. Nature **415:**331–335. http://dx.doi.org/10.1038/415331a.
4. **Patterson LJ.** 2011. The "STEP-wise" future of adenovirus-based HIV

vaccines. Curr Med Chem **18:**3981–3986. http://dx.doi.org/10.2174/092986711796957211.

5. **Buchbinder SP, Mehrotra DV, Duerr A, Fitzgerald DW, Mogg R, Li D, Gilbert PB, Lama JR, Marmor M, Del Rio C, McElrath MJ, Casimiro DR, Gottesdiener KM, Chodakewitz JA, Corey L, Robertson MN, Step Study Protocol Team.** 2008. Efficacy assessment of a cell-mediated immunity HIV-1 vaccine (the Step Study): a double-blind, randomised, placebo-controlled, test-of-concept trial. Lancet **372:**1881–1893. http://dx.doi.org/10.1016/S0140-6736(08)61591-3.
6. **Gray GE, Allen M, Moodie Z, Churchyard G, Bekker LG, Nchabeleng M, Mlisana K, Metch B, de Bruyn G, Latka MH, Roux S, Mathebula M, Naicker N, Ducar C, Carter DK, Puren A, Eaton N, McElrath MJ, Robertson M, Corey L, Kublin JG, HVTN 503/Phambili Study Team.** 2011. Safety and efficacy of the HVTN 503/Phambili study of a clade-B-based HIV-1 vaccine in South Africa: a double-blind, randomised, placebo-controlled test-of-concept phase 2b study. Lancet Infect Dis **11:**507–515. http://dx.doi.org/10.1016/S1473-3099(11)70098-6.
7. **Gray GE, Moodie Z, Metch B, Gilbert PB, Bekker LG, Churchyard G, Nchabeleng M, Mlisana K, Laher F, Roux S, Mngadi K, Innes C, Mathebula M, Allen M, McElrath MJ, Robertson M, Kublin J, Corey L, HVTN 503/Phambili Study Team.** 2014. Recombinant adenovirus type 5 HIV gag/pol/nef vaccine in South Africa: unblinded, long-term follow-up of the phase 2b HVTN 503/Phambili study. Lancet Infect Dis **14:**388–396. http://dx.doi.org/10.1016/S1473-3099(14)70020-9.
8. **Hammer SM, Sobieszczyk ME, Janes H, Karuna ST, Mulligan MJ, Grove D, Koblin BA, Buchbinder SP, Keefer MC, Tomaras GD, Frahm N, Hural J, Anude C, Graham BS, Enama ME, Adams E, DeJesus E, Novak RM, Frank I, Bentley C, Ramirez S, Fu R, Koup RA, Mascola JR, Nabel GJ, Montefiori DC, Kublin J, McElrath MJ, Corey L, Gilbert PB, HVTN 505 Study Team.** 2013. Efficacy trial of a DNA/rAd5 HIV-1 preventive vaccine. N Engl J Med **369:**2083–2092. http://dx.doi.org/10.1056/NEJMoa1310566.
9. **Rerks-Ngarm S, Pitisuttithum P, Nitayaphan S, Kaewkungwal J, Chiu J, Paris R, Premsri N, Namwat C, de Souza M, Adams E, Benenson M, Gurunathan S, Tartaglia J, McNeil JG, Francis DP, Stablein D, Birx DL, Chunsuttiwat S, Khamboonruang C, Thongcharoen P, Robb ML, Michael NL, Kunasol P, Kim JH, MOPH-TAVEG Investigators.** 2009. Vaccination with ALVAC and AIDSVAX to prevent HIV-1 infection in Thailand. N Engl J Med **361:**2209–2220. http://dx.doi.org/10.1056/NEJMoa0908492.
10. **Johnson JA, Barouch DH, Baden LR.** 2013. Nonreplicating vectors in HIV vaccines. Curr Opin HIV AIDS **8:**412–420. http://dx.doi.org/10.1097/COH.0b013e328363d3b7.
11. **Esteban M.** 2009. Attenuated poxvirus vectors MVA and NYVAC as promising vaccine candidates against HIV/AIDS. Hum Vaccin **5:**867–871. http://dx.doi.org/10.4161/hv.9693.
12. **Tartaglia J, Perkus ME, Taylor J, Norton EK, Audonnet JC, Cox WI, Davis SW, van der Hoeven J, Meignier B, Riviere M, Languet B, Paoletti E.** 1992. NYVAC: a highly attenuated strain of vaccinia virus. Virology **188:**217–232. http://dx.doi.org/10.1016/0042-6822(92)90752-B.
13. **Garcia-Arriaza J, Esteban M.** 2014. Enhancing poxvirus vectors vaccine immunogenicity. Hum Vaccin Immunother **10:**2235–2244. http://dx.doi.org/10.4161/hv.28974.
14. **Bart PA, Goodall R, Barber T, Harari A, Guimaraes-Walker A, Khonkarly M, Sheppard NC, Bangala Y, Frachette MJ, Wagner R, Liljestrom P, Kraehenbuhl JP, Girard M, Goudsmit J, Esteban M, Heeney J, Sattentau Q, McCormack S, Babiker A, Pantaleo G, Weber J,** EuroVacc Consortium. 2008. EV01: a phase I trial in healthy HIV negative volunteers to evaluate a clade C HIV vaccine, NYVAC-C undertaken by the EuroVacc Consortium. Vaccine **26:**3153–3161. http://dx.doi.org/10.1016/j.vaccine.2008.03.083.
15. **Harari A, Bart PA, Stohr W, Tapia G, Garcia M, Medjitna-Rais E, Burnet S, Cellerai C, Erlwein O, Barber T, Moog C, Liljestrom P, Wagner R, Wolf H, Kraehenbuhl JP, Esteban M, Heeney J, Frachette MJ, Tartaglia J, McCormack S, Babiker A, Weber J, Pantaleo G.** 2008. An HIV-1 clade C DNA prime, NYVAC boost vaccine regimen induces reliable, polyfunctional, and long-lasting T cell responses. J Exp Med **205:**63–77. http://dx.doi.org/10.1084/jem.20071331.
16. **Mooij P, Balla-Jhagjhoorsingh SS, Koopman G, Beenhakker N, van Haaften P, Baak I, Nieuwenhuis IG, Kondova I, Wagner R, Wolf H, Gomez CE, Najera JL, Jimenez V, Esteban M, Heeney JL.** 2008. Differential $CD4^+$ versus $CD8^+$ T-cell responses elicited by different poxvirus-based human immunodeficiency virus type 1 vaccine candidates provide comparable efficacies in primates. J Virol **82:**2975–2988. http://dx.doi.org/10.1128/JVI.02216-07.
17. **Harari A, Rozot V, Cavassini M, Enders FB, Vigano S, Tapia G, Castro E, Burnet S, Lange J, Moog C, Garin D, Costagliola D, Autran B, Pantaleo G, Bart PA.** 2012. NYVAC immunization induces polyfunctional HIV-specific T-cell responses in chronically-infected, ART-treated HIV patients. Eur J Immunol **42:**3038–3048. http://dx.doi.org/10.1002/eji.201242696.
18. **Perreau M, Welles HC, Harari A, Hall O, Martin R, Maillard M, Dorta G, Bart PA, Kremer EJ, Tartaglia J, Wagner R, Esteban M, Levy Y, Pantaleo G.** 2011. DNA/NYVAC vaccine regimen induces HIV-specific CD4 and CD8 T-cell responses in intestinal mucosa. J Virol **85:**9854–9862. http://dx.doi.org/10.1128/JVI.00788-11.
19. **Gomez CE, Najera JL, Krupa M, Perdiguero B, Esteban M.** 2011. MVA and NYVAC as vaccines against emergent infectious diseases and cancer. Curr Gene Ther **11:**189–217. http://dx.doi.org/10.2174/156652311795684731.
20. **Gomez CE, Perdiguero B, Najera JL, Sorzano CO, Jimenez V, Gonzalez-Sanz R, Esteban M.** 2012. Removal of vaccinia virus genes that block interferon type I and II pathways improves adaptive and memory responses of the HIV/AIDS vaccine candidate NYVAC-C in mice. J Virol **86:**5026–5038. http://dx.doi.org/10.1128/JVI.06684-11.
21. **Delaloye J, Roger T, Steiner-Tardivel QG, Le Roy D, Knaup Reymond M, Akira S, Petrilli V, Gomez CE, Perdiguero B, Tschopp J, Pantaleo G, Esteban M, Calandra T.** 2009. Innate immune sensing of modified vaccinia virus Ankara (MVA) is mediated by TLR2-TLR6, MDA-5 and the NALP3 inflammasome. PLoS Pathog **5:**e1000480. http://dx.doi.org/10.1371/journal.ppat.1000480.
22. **Kibler KV, Gomez CE, Perdiguero B, Wong S, Huynh T, Holechek S, Arndt W, Jimenez V, Gonzalez-Sanz R, Denzler K, Haddad EK, Wagner R, Sekaly RP, Tartaglia J, Pantaleo G, Jacobs BL, Esteban M.** 2011. Improved NYVAC-based vaccine vectors. PLoS One **6:**e25674. http://dx.doi.org/10.1371/journal.pone.0025674.
23. **Gomez CE, Perdiguero B, Garcia-Arriaza J, Esteban M.** 2012. Poxvirus vectors as HIV/AIDS vaccines in humans. Hum Vaccin Immunother **8:**1192–1207. http://dx.doi.org/10.4161/hv.20778.
24. **Caskey M, Lefebvre F, Filali-Mouhim A, Cameron MJ, Goulet JP, Haddad EK, Breton G, Trumpfheller C, Pollak S, Shimeliovich I, Duque-Alarcon A, Pan L, Nelkenbaum A, Salazar AM, Schlesinger SJ, Steinman RM, Sekaly RP.** 2011. Synthetic double-stranded RNA induces innate immune responses similar to a live viral vaccine in humans. J Exp Med **208:**2357–2366. http://dx.doi.org/10.1084/jem.20111171.
25. **Gentleman RC, Carey VJ, Bates DM, Bolstad B, Dettling M, Dudoit S, Ellis B, Gautier L, Ge Y, Gentry J, Hornik K, Hothorn T, Huber W, Iacus S, Irizarry R, Leisch F, Li C, Maechler M, Rossini AJ, Sawitzki G, Smith C, Smyth G, Tierney L, Yang JY, Zhang J.** 2004. Bioconductor: open software development for computational biology and bioinformatics. Genome Biol **5:**R80. http://dx.doi.org/10.1186/gb-2004-5-10-r80.
26. **Evans VA, Kumar N, Filali A, Procopio FA, Yegorov O, Goulet JP, Saleh S, Haddad EK, da Fonseca Pereira C, Ellenberg PC, Sekaly RP, Cameron PU, Lewin SR.** 2013. Myeloid dendritic cells induce HIV-1 latency in non-proliferating CD4+ T cells. PLoS Pathog **9:**e1003799. http://dx.doi.org/10.1371/journal.ppat.1003799.
27. **Waddell SJ, Popper SJ, Rubins KH, Griffiths MJ, Brown PO, Levin M, Relman DA.** 2010. Dissecting interferon-induced transcriptional programs in human peripheral blood cells. PLoS One **5:**e9753. http://dx.doi.org/10.1371/journal.pone.0009753.
28. **Roger T, Glauser MP, Calandra T.** 2001. Macrophage migration inhibitory factor (MIF) modulates innate immune responses induced by endotoxin and Gram-negative bacteria. J Endotoxin Res **7:**456–460. http://dx.doi.org/10.1177/09680519010070061101.
29. **Cheong C, Matos I, Choi JH, Dandamudi DB, Shrestha E, Longhi MP, Jeffrey KL, Anthony RM, Kluger C, Nchinda G, Koh H, Rodriguez A, Idoyaga J, Pack M, Velinzon K, Park CG, Steinman RM.** 2010. Microbial stimulation fully differentiates monocytes to DC-SIGN/CD209(+) dendritic cells for immune T cell areas. Cell **143:**416–429. http://dx.doi.org/10.1016/j.cell.2010.09.039.
30. **Liu M, Guo S, Hibbert JM, Jain V, Singh N, Wilson NO, Stiles JK.** 2011. CXCL10/IP-10 in infectious diseases pathogenesis and potential therapeutic implications. Cytokine Growth Factor Rev **22:**121–130. http://dx.doi.org/10.1016/j.cytogfr.2011.06.001.
31. **Chawla-Sarkar M, Lindner DJ, Liu YF, Williams BR, Sen GC, Silverman RH, Borden EC.** 2003. Apoptosis and interferons: role of interferon-

stimulated genes as mediators of apoptosis. Apoptosis **8:**237–249. http://dx.doi.org/10.1023/A:1023668705040.
32. **Deveraux QL, Reed JC.** 1999. IAP family proteins—suppressors of apoptosis. Genes Dev **13:**239–252. http://dx.doi.org/10.1101/gad.13.3.239.
33. **Kanneganti TD.** 2010. Central roles of NLRs and inflammasomes in viral infection. Nat Rev Immunol **10:**688–698. http://dx.doi.org/10.1038/nri2851.
34. **Venkatesh D, Ernandez T, Rosetti F, Batal I, Cullere X, Luscinskas FW, Zhang Y, Stavrakis G, Garcia-Cardena G, Horwitz BH, Mayadas TN.** 2013. Endothelial TNF receptor 2 induces IRF1 transcription factor-dependent interferon-beta autocrine signaling to promote monocyte recruitment. Immunity **38:**1025–1037. http://dx.doi.org/10.1016/j.immuni.2013.01.012.
35. **Yarilina A, Park-Min KH, Antoniv T, Hu X, Ivashkiv LB.** 2008. TNF activates an IRF1-dependent autocrine loop leading to sustained expression of chemokines and STAT1-dependent type I interferon-response genes. Nat Immunol **9:**378–387. http://dx.doi.org/10.1038/ni1576.
36. **Alcami A, Smith GL.** 1995. Vaccinia, cowpox, and camelpox viruses encode soluble gamma interferon receptors with novel broad species specificity. J Virol **69:**4633–4639.
37. **Mossman K, Nation P, Macen J, Garbutt M, Lucas A, McFadden G.** 1996. Myxoma virus M-T7, a secreted homolog of the interferon-gamma receptor, is a critical virulence factor for the development of myxomatosis in European rabbits. Virology **215:**17–30. http://dx.doi.org/10.1006/viro.1996.0003.
38. **Mossman K, Upton C, Buller RM, McFadden G.** 1995. Species specificity of ectromelia virus and vaccinia virus interferon-gamma binding proteins. Virology **208:**762–769. http://dx.doi.org/10.1006/viro.1995.1208.
39. **Mossman K, Upton C, McFadden G.** 1995. The myxoma virus-soluble interferon-gamma receptor homolog, M-T7, inhibits interferon-gamma in a species-specific manner. J Biol Chem **270:**3031–3038. http://dx.doi.org/10.1074/jbc.270.7.3031.
40. **Symons JA, Tscharke DC, Price N, Smith GL.** 2002. A study of the vaccinia virus interferon-gamma receptor and its contribution to virus virulence. J Gen Virol **83:**1953–1964.
41. **Colamonici OR, Domanski P, Sweitzer SM, Larner A, Buller RM.** 1995. Vaccinia virus B18R gene encodes a type I interferon-binding protein that blocks interferon alpha transmembrane signaling. J Biol Chem **270:**15974–15978. http://dx.doi.org/10.1074/jbc.270.27.15974.
42. **Waibler Z, Anzaghe M, Frenz T, Schwantes A, Pohlmann C, Ludwig H, Palomo-Otero M, Alcami A, Sutter G, Kalinke U.** 2009. Vaccinia virus-mediated inhibition of type I interferon responses is a multifactorial process involving the soluble type I interferon receptor B18 and intracellular components. J Virol **83:**1563–1571. http://dx.doi.org/10.1128/JVI.01617-08.
43. **Quakkelaar ED, Redeker A, Haddad EK, Harari A, McCaughey SM, Duhen T, Filali-Mouhim A, Goulet JP, Loof NM, Ossendorp F, Perdiguero B, Heinen P, Gomez CE, Kibler KV, Koelle DM, Sekaly RP, Sallusto F, Lanzavecchia A, Pantaleo G, Esteban M, Tartaglia J, Jacobs BL, Melief CJ.** 2011. Improved innate and adaptive immunostimulation by genetically modified HIV-1 protein expressing NYVAC vectors. PLoS One **6:**e16819. http://dx.doi.org/10.1371/journal.pone.0016819.
44. **Roberts TL, Idris A, Dunn JA, Kelly GM, Burnton CM, Hodgson S, Hardy LL, Garceau V, Sweet MJ, Ross IL, Hume DA, Stacey KJ.** 2009. HIN-200 proteins regulate caspase activation in response to foreign cytoplasmic DNA. Science **323:**1057–1060. http://dx.doi.org/10.1126/science.1169841.
45. **Fernandes-Alnemri T, Yu JW, Datta P, Wu J, Alnemri ES.** 2009. AIM2 activates the inflammasome and cell death in response to cytoplasmic DNA. Nature **458:**509–513. http://dx.doi.org/10.1038/nature07710.
46. **Hornung V, Ablasser A, Charrel-Dennis M, Bauernfeind F, Horvath G, Caffrey DR, Latz E, Fitzgerald KA.** 2009. AIM2 recognizes cytosolic dsDNA and forms a caspase-1-activating inflammasome with ASC. Nature **458:**514–518. http://dx.doi.org/10.1038/nature07725.
47. **Burckstummer T, Baumann C, Bluml S, Dixit E, Durnberger G, Jahn H, Planyavsky M, Bilban M, Colinge J, Bennett KL, Superti-Furga G.** 2009. An orthogonal proteomic-genomic screen identifies AIM2 as a cytoplasmic DNA sensor for the inflammasome. Nat Immunol **10:**266–272. http://dx.doi.org/10.1038/ni.1702.
48. **Poeck H, Bscheider M, Gross O, Finger K, Roth S, Rebsamen M, Hannesschlager N, Schlee M, Rothenfusser S, Barchet W, Kato H, Akira S, Inoue S, Endres S, Peschel C, Hartmann G, Hornung V, Ruland J.** 2010. Recognition of RNA virus by RIG-I results in activation of CARD9 and inflammasome signaling for interleukin 1 beta production. Nat Immunol **11:**63–69. http://dx.doi.org/10.1038/ni.1824.
49. **Rathinam VA, Jiang Z, Waggoner SN, Sharma S, Cole LE, Waggoner L, Vanaja SK, Monks BG, Ganesan S, Latz E, Hornung V, Vogel SN, Szomolanyi-Tsuda E, Fitzgerald KA.** 2010. The AIM2 inflammasome is essential for host defense against cytosolic bacteria and DNA viruses. Nat Immunol **11:**395–402. http://dx.doi.org/10.1038/ni.1864.
50. **Ray CA, Black RA, Kronheim SR, Greenstreet TA, Sleath PR, Salvesen GS, Pickup DJ.** 1992. Viral inhibition of inflammation: cowpox virus encodes an inhibitor of the interleukin-1beta converting enzyme. Cell **69:**597–604. http://dx.doi.org/10.1016/0092-8674(92)90223-Y.
51. **Komiyama T, Ray CA, Pickup DJ, Howard AD, Thornberry NA, Peterson EP, Salvesen G.** 1994. Inhibition of interleukin-1beta converting enzyme by the cowpox virus serpin CrmA. An example of cross-class inhibition. J Biol Chem **269:**19331–19337.
52. **Guarda G, Braun M, Staehli F, Tardivel A, Mattmann C, Forster I, Farlik M, Decker T, Du Pasquier RA, Romero P, Tschopp J.** 2011. Type I interferon inhibits interleukin-1 production and inflammasome activation. Immunity **34:**213–223. http://dx.doi.org/10.1016/j.immuni.2011.02.006.
53. **Inoue M, Williams KL, Oliver T, Vandenabeele P, Rajan JV, Miao EA, Shinohara ML.** 2012. Interferon-β therapy against EAE is effective only when development of the disease depends on the NLRP3 inflammasome. Sci Signal **5:**ra38. http://dx.doi.org/10.1126/scisignal.2002767.
54. **Veeranki S, Duan X, Panchanathan R, Liu H, Choubey D.** 2011. IFI16 protein mediates the anti-inflammatory actions of the type-I interferons through suppression of activation of caspase-1 by inflammasomes. PLoS One **6:**e27040. http://dx.doi.org/10.1371/journal.pone.0027040.
55. **Kerur N, Veettil MV, Sharma-Walia N, Bottero V, Sadagopan S, Otageri P, Chandran B.** 2011. IFI16 acts as a nuclear pathogen sensor to induce the inflammasome in response to Kaposi sarcoma-associated herpesvirus infection. Cell Host Microbe **9:**363–375. http://dx.doi.org/10.1016/j.chom.2011.04.008.
56. **Masters SL, Mielke LA, Cornish AL, Sutton CE, O'Donnell J, Cengia LH, Roberts AW, Wicks IP, Mills KH, Croker BA.** 2010. Regulation of interleukin-1beta by interferon-gamma is species specific, limited by suppressor of cytokine signalling 1 and influences interleukin-17 production. EMBO Rep **11:**640–646. http://dx.doi.org/10.1038/embor.2010.93.
57. **Bauernfeind FG, Horvath G, Stutz A, Alnemri ES, MacDonald K, Speert D, Fernandes-Alnemri T, Wu J, Monks BG, Fitzgerald KA, Hornung V, Latz E.** 2009. Cutting edge: NF-kappaB activating pattern recognition and cytokine receptors license NLRP3 inflammasome activation by regulating NLRP3 expression. J Immunol **183:**787–791. http://dx.doi.org/10.4049/jimmunol.0901363.
58. **Latz E, Xiao TS, Stutz A.** 2013. Activation and regulation of the inflammasomes. Nat Rev Immunol **13:**397–411. http://dx.doi.org/10.1038/nri3452.
59. **Roth S, Rottach A, Lotz-Havla AS, Laux V, Muschaweckh A, Gersting SW, Muntau AC, Hopfner KP, Jin L, Vanness K, Petrini JH, Drexler I, Leonhardt H, Ruland J.** 2014. Rad50-CARD9 interactions link cytosolic DNA sensing to IL-1beta production. Nat Immunol **15:**538–545. http://dx.doi.org/10.1038/ni.2888.
60. **Madera RF, Wang JP, Libraty DH.** 2011. The combination of early and rapid type I IFN, IL-1alpha, and IL-1beta production are essential mediators of RNA-like adjuvant driven CD4+ Th1 responses. PLoS One **6:**e29412. http://dx.doi.org/10.1371/journal.pone.0029412.
61. **Ramos HJ, Lanteri MC, Blahnik G, Negash A, Suthar MS, Brassil MM, Sodhi K, Treuting PM, Busch MP, Norris PJ, Gale M, Jr.** 2012. IL-1beta signaling promotes CNS-intrinsic immune control of West Nile virus infection. PLoS Pathog **8:**e1003039. http://dx.doi.org/10.1371/journal.ppat.1003039.
62. **Wilson EB, Yamada DH, Elsaesser H, Herskovitz J, Deng J, Cheng G, Aronow BJ, Karp CL, Brooks DG.** 2013. Blockade of chronic type I interferon signaling to control persistent LCMV infection. Science **340:**202–207. http://dx.doi.org/10.1126/science.1235208.
63. **Teijaro JR, Ng C, Lee AM, Sullivan BM, Sheehan KC, Welch M, Schreiber RD, de la Torre JC, Oldstone MB.** 2013. Persistent LCMV infection is controlled by blockade of type I interferon signaling. Science **340:**207–211. http://dx.doi.org/10.1126/science.1235214.
64. **Sandler NG, Bosinger SE, Estes JD, Zhu RT, Tharp GK, Boritz E, Levin D, Wijeyesinghe S, Makamdop KN, Del Prete GQ, Hill BJ, Timmer JK, Reiss E, Yarden G, Darko S, Contijoch E, Todd JP, Silvestri G, Nason M, Norgren RB, Jr, Keele BF, Rao S, Langer JA, Lifson JD, Schreiber G, Douek DC.** 2014. Type I interferon responses in rhesus macaques prevent SIV infection and slow disease progression. Nature **511:**601–605. http://dx.doi.org/10.1038/nature13554.